Development of an Aqueous Ammonia Based PCC Technology for Australian Conditions

Process modelling of combined SO_2 and CO_2 capture using aqueous ammonia

Hai Yu

CSIRO Energy Technology

PO Box 330, Newcastle, NSW 2300, Australia

Lichun Li, Marcel Maeder

Department of Chemistry, University of Newcastle, Callaghan, NSW 2308, Australia

Kangkang Li, Moses Tade

Department of Chemical Engineering, Curtin University of Technology

Project Number: **3-0911-0142**

Project Start Date: **15/06/2012**

Project End date: **30/09/2015**

The Report Period: **30/03/2013 - 30/09/2014**

Copyright and disclaimer

Important disclaimer

Acknowledgement

The authors wish to acknowledge financial assistance provided through both CSIRO Energy Flagship and Australian National Low Emissions Coal Research and Development (ANLEC R&D). ANLEC R&D is supported by Australian Coal Association Low Emissions Technology Limited and the Australian Government through the Clean Energy Initiative. The authors are also grateful to Dr Allen Lowe and Mr Anthony Callen for review of this report and providing comments and suggestions.

Table of Contents

List of Figures

List of Tables

1 Executive Summary

This research project focuses on the development of the advanced aqueous ammonia (NH_3) based post combustion capture (PCC) technology for significant reduction of CO_2 emission from coal fired power stations in Australia.

Currently, the commercially available PCC technology is mainly based on alkanol/alkyl amine solutions. This technology will reduce the power plant efficiency by 25-30% and involve significant capital/investment costs including the expensive flue gas desulfurization which is not installed in Australian power plants. As a promising solvent, aqueous ammonia has many advantages over amine-based capture technologies, including no degradation in the presence of O_2, a higher CO_2 absorption capacity than monoethanolamine (MEA), a low regeneration energy. It also has a potential to capture oxides of nitrogen (NO_x) and sulphur dioxide (SO_2) from the flue gas of coal-fired power plants, and to produce value-added chemicals, such as ammonium sulfate and ammonium nitrate, which are commonly used as fertiliser.

This research project is based on CSIRO PCC pilot plant trials with an aqueous ammonia based liquid absorbent under real flue gas conditions in a $7M AUD pilot plant at Delta Electricity's Munmorah power station and ongoing work in this area. The pilot plant trials have confirmed the technical feasibility of the process and confirmed some of the expected benefits. The pilot plant trials have also highlighted some of the issues when using aqueous ammonia in a PCC process. These include a relatively low CO_2 absorption rate and high ammonia loss. These issues currently limit the economical feasibility of the aqueous ammonia based PCC process.

The strategy of the research proposed here is to extend a number of novel approaches developed previously by CSIRO to address the issues identified and make the process economically favourable. These novel approaches to be further explored in this project include promotion of CO_2 absorption rate through the introduction of additives, combined removal of SO_2 and CO_2 and recovery of ammonia, and absorption under pressure to further enhance CO_2 absorption and suppress ammonia loss. In addition, the research project will combine an experimental and modelling approach to develop a rigorous rate based model for the aqueous ammonia based capture process which allows for reliable process simulation, optimisation and scale up. The outcomes of this research project will include the demonstration of the advanced aqueous ammonia based PCC at a CO_2 capture rate of at least 10 kg/h with CSIRO's process development facility in Newcastle. The advanced technology is expected to achieve a CO_2 absorption rate that is comparable with the standard MEA based solution, limit the power plant efficiency loss below 20%, and achieve the combined removal of SO_2 and recovery of ammonia to produce ammonium sulphate and eliminate additional flue gas desulfurization and reduce wash water consumption. The combined outcomes will enable the advanced technology to achieve a significant reduction in incremental levelised cost of electricity compared to state of the art, advanced amine based PCC technology.

This project is planned over a three-year time frame and is divided into 6 stages. This report summaries the progress of the projects and presents the results obtained in stage 4.

A rigorous rate-based model for the system of NH_3-CO_2-SO_2-H_2O was developed in Aspen Plus® and validated by the experimental results from open literature and pilot plant trials at Munmorah Power Station. The model can satisfactorily predict the CO_2 absorption, CO_2desorption and SO_2 removal in packed columns.

We have proposed a novel and effective process for the combined SO_2 removal and ammonia recycle, which can be integrated with the aqueous ammonia based CO_2 capture process to achieve flue gas cooling, SO_2 and CO_2 removal and ammonia recycle simultaneously in one process. The process simulation using the rated-based model showed that under the typical flue gas conditions, the proposed process has a SO_2 removal efficiency of over 99.9% and an ammonia reuse efficiency of 99.9%. The novel process can not only simplify the flue gas desulfurization, but also resolve the problems of ammonia loss and SO_2 removal, thus holding the potential of cutting the CO_2 capture costs significantly. The separate experiments on SO_2 and ammonia absorption using a bubble column were carried out to further evaluate the technical feasibility of the combined process. The experimental results qualitatively confirmed the simulated results and the technical feasibility of the process.

The amino acid salts studied in this work can significantly enhance CO_2 absorption in aqueous ammonia at low CO_2 loadings but their role in promotion of CO_2 absorption rate becomes much smaller with an increase in CO_2 loading. The mass transfer coefficients of CO_2 in amino acid salts and ammonia mixtures are close to those in MEA but generally lower under the conditions studied. In comparison, ammonia mixed with piperazine or 2-methyl piperazine can achieve mass transfer coefficients higher than those in MEA.

In an attempt to develop a rate-based model for the promoted ammonia solvents which is not available in Aspen Plus, we used an in-house software tool implemented in the Matlab® to model the mass transfer of CO_2 in the ammonia and piperazine mixtures in a wetted wall column. The software tool incorporates the reaction kinetic model developed from stopped flow kinetic study and solves partial differential equations and nonlinear simultaneous equations that define the diffusion, reaction and equilibrium processes occurring in a thin liquid film. It has been found that both calculated and experimental mass transfer coefficients increases with the concentration of piperazine added to the blended ammonia/piperazine solutions with constant ammonia and CO_2 concentrations in solutions. However, the calculated values underestimate the measured values by a relative error of approximately 30-40%. Further investigation is required to understand the reasons for the discrepancy and improve the mass transfer simulations.

The milestones of the project for the report period have been achieved and the project is on track to achieve the milestones which are due on 30 March 2015.

2 Recent Advancement of Solvent Development for Post-Combustion Capture

Post combustion capture (PCC) is a process that uses an aqueous absorption liquid incorporating compounds such as ammonia or amine to capture CO_2 from power station flue gases and many other industrial sources. It is the leading capture technology as a result of the potential benefits, such as,

- It can be retrofitted to existing power plants or integrated with new infrastructure to achieve a range of CO_2 reductions, from partial retrofit to full capture capacity;
- It has a lower technology risk compared with other competing technologies;
- Renewable technologies can be integrated with PCC, for example, low cost solar thermal collectors can provide the heat required to separate CO_2 from solvents;
- PCC can be used to capture CO_2 from a range of sources – smelters, kilns and steel works, as well as coal- and gas-fired power stations.

Currently, the commercially available PCC technology is mainly based on alkanol/alkyl amine solutions. A study by Dave et al. shows that retrofitting a monoethanolamine (MEA) based PCC plant to the existing/new mechanical draft water cooled black coal fired plants will reduce the power plant efficiency by 10 absolute percentage points and involves significant capital investment costs (Dave et al., 2011). The research work has been intensified in recent years to improve the existing solvents or developed novel solvents to reduce the capital and running costs of the PCC technologies. The report from Global CCS institute summaries the status of near term PCC technologies up to Jan 2012 (Global CCS Institute, 2012). This report provides an update on the recent development of these near term technologies.

Table 1 An update on recent development of the near term post combustion CO_2 capture technologies

Technology provider	Solvent	Comments
Cansolv	Cansolv chemical solvents	As part of a retrofit of SaskPower's Boundary Dam 3 unit, a post combustion carbon dioxide (CO_2) capture facility based on Cansolv chemical solvent will be installed to capture up to 1 million metric tons per annum (Mtpa) of CO_2 . Captured CO_2 in excess of that to be delivered to oil fields for enhanced oil recovery will be injected into a deep saline formation as part of the Aquistore Project. Mechanical completion of the carbon capture facilities was in December 2013 with commissioning activities beginning thereafter. The completion of the power plant refurbishment occurred in the second quarter of 2014. Overall operation of the Demonstration Project is planned for late in the second quarter or early third quarter of 2014 (Boundary dam, 2014). In addition, Cansolv has recently developed a new solvent, DC-201. Pilot plant trials showed the new solvent can achieve a reduction of regeneration energy consumption by 35% compared to MEA. The new solvent will be tested in Cansolv SO_2 CO_2 Demonstrated Plant in Wales, UK (Just, 2013).
Fluor	Econamine FG Plus	Fluor's Econamine FG Plus^{SM} technology is claimed to reduce steam consumption by over 30% compared to 'generic' MEA technology and has been used in more than 25 commercial plants for the recovery of CO_2 from

		flue gas at rates from 6 to 1000 metric tons per day. The flue gas processed was mainly produced by combustion of natural gas; four units use flue gas from natural gas steam reformers. Recently Fluor's Econamine FG Plus^{SM} technology has been applied to demonstrate removal of carbon dioxide from flue gas at E.ON's Wilhelmshaven coal-fired power plant. The Wilhelmshaven carbon capture pilot plant is designed for capturing 70 metric tons per day when operating at full capacity. The plant has been operated since October 2012. Over 1,400 hours of operation had been achieved by January 2013 (Reddy et al., 2013).
MHI	KS-1 sterically hindered amine solvent	MHI KM-CDR process was employed in the world's first integrated CCS project for flue gas from a coal-fired power plant. The CO_2 capture facility, which was built jointly by MHI and Southern Company, is the world's largest in scale and is able to capture 500 metric tons per day, with CO_2 recovery efficiency above 90%. (Hirata et al., 2013). The captured and compressed CO2 has been injected since August, 2012. As of October 2013 the plant had operated for a cumulative 10,600 hrs and during that time achieved 198,000 tonnes of CO_2 captured and 101,700 tons of CO_2 stored (Hirata, 2014). NRG Energy and JX Nippon Oil & Gas Exploration are jointly carrying out Petra Nova Carbon Capture Project at W.A. Parish power plant at Thompsons, near Houston, Texas. The WA Parish project will utilize the KM-CDR Process and uses a proprietary KS-1 high-performance solvent for the CO_2 absorption and desorption. The CO_2 capture capacity is 1.4 million tonnes per annum. The plant is expected to be operational in 2016. (Petra Nova, 2014) MHI claims that KM-CDR circulation rate is 60% of that for (unspecified) MEA, regeneration energy is 68% of MEA, and solvent loss and degradation are 10% of MEA. MHI is working on process improvements that are said to have potential to reduce the regeneration heat requirement to 1860 kJ/kg CO_2 from 2790 kJ/kg CO_2 (Global CCS Institute, 2012).
Alstom Power	Aqueous ammonia	Alstom conducted a number of field tests of chilled ammonia process (CAP) and completed the demonstration project at American Electric Power's Mountaineer Plant at end of May 2011 after a 21 month period The results shows the heat requirement of 2.2 MJ/kg CO_2 captured for the chilled ammonia process (Jönssona and Telikapalli, 2012). Gassnova awarded Alstom a concept study for a full-scale CO_2 capture plant to be located at Mongstad near Bergen, Norway. The Alstom test plant recently commissioned at TCM continues the overall validation programme for CAP. CAP operation at TCM tuning first results is: CO_2 capture rates from 80% to as high as 87%, CO_2 purity of greater than 99.9%, low NH_3 emissions (Lombardo G., 2014).
Alstom Power	Advanced amine solvent	Dow Oil & Gas and Alstom are jointly developing advanced amine process (AAP) technology that utilizes UCARSOL™ FGC 3000, an advanced amine solvent from Dow, in combination with advanced flow schemes to provide a cost-effective post-combustion, carbon capture technology for application in power plants worldwide. The carbon capture demonstration plant was located at the EDF thermal power plant in Le Havre, France, and captured its first tonne of CO_2 in July 2013. The test programme was completed in March 2014. The technology has successfully been demonstrated in the field at > 99.9% pure CO2 product quality at 90% capture rates. The AAP design has been optimized for emissions mitigation and control and has less solvent degradation as compared to Monoethanolamine (MEA) solvent (Baburao, 2014).
Babcock & Wilcox	OptiCap^{TM}	Babcock & Wilcox Power Generation Group, Inc. (B&W PGG) completed a three months test campaign from September 2011 to December 2011 using OptiCap solvent. The test run spanned approximately 2,000 hours. The OptiCap solvent has many benefits including low corrosivity, low regeneration energy, and an expected high resistance to solvent degradation.

		The lowest OptiCap regeneration energy measured was 2.55 MJ/Kg CO_2. In addition, it offers the ability to operate the capture process at elevated pressures due to its thermal stability, which will have a significant favourable impact on mechanical compression energy (Gayheart, 2013).
Aker Clean carbon (ACC)	ACC proprietary solvents	ACC has been testing its solvent on the CO_2 technology Centre Mongstad since 2012. The test campaigns have shown that ACC advanced solvents S21 and S26 show good energy performance and are superior to 30 wt% MEA with respect to solvent degradation, ammonia emission and nitrosamine formation. For example, the reboiler duty for solvents S21 and S26 was found to be approximately 10% lower than that for MEA. Solvent amine losses have been quantified to approximately 2.6 kg amine/ton CO_2 captured for MEA, 0.5-0.6 kg amine/ton CO_2 captured for ACCTM advanced solvent S21, and 0.2-0.3 kg amine/ton CO_2 captured for ACCTM advanced solvent S26 (Gorset, 2014).

In addition to further development of the near term technologies, intensive research work has been carried out to develop novel solvents. The focus of these researchers is primarily on increase in absorption capacity and reduction of energy consumption of the solvents. These novel solvents include ionic liquids, enzyme catalysed solvents, and phase change solvents. The novel solvents mentioned above are still at the early stage development and have not been tested in the pilot plant under the real flue gas conditions.

References

Baburao B., et al., 2014. Advanced amine process technology operations and results from demonstration facility at EDF Le Havre, to be presented in the 12nd International Conference on Greenhouse Gas Control Technologies (GHGT 12).

Boundary dam Integrated carbon capture and sequestration demonstration project, http://www.globalccsinstitute.com/project/boundary-dam-integrated-carbon-capture-and-sequestration-demonstration-project, access on 24 September 2014.

Dave, N., Do, T., Palfreyman, D., and Feron, P. H. M., 2011. Impact of liquid absorption process development on the costs of post-combustion capture in Australian coal-fired power stations, Chemical Engineering Research & Design, 89, 1625-1638.

Gayheart, J. W., Moorman, S. A., Parsons, T. R., and Poling, C. W. ,2013. Babcock & Wilcox Power Generation Group, Inc.'s RSAT™ process and field demonstration of the OptiCap™ advanced solvent at the US-DOE's National Carbon Capture Center, Energy Procedia, 37, 1951-1967.

Global CCS Institute, 2012. CO_2 capture technologies - post combustion capture (PCC), http://www.globalccsinstitute.com/publications/co_2-capture-technologies-post-combustion-capture-pcc.

Gorset, O., et al., 2014. Results from testing of Aker Solutions advanced amine solvents at CO_2 Technology Centre Mongstad, to be presented in the 12nd International Conference on Greenhouse Gas Control Technologies (GHGT 12).

Hirata, T., Nagayasu, H., Kamijo, T., Kubota, Y., Tsujiuchi, T., Yonekawa, T., Wood, P., Ivie Ii, M. A., and Nick, I. P. E.,2013. Project update of 500 TPD demonstration plant for coal-fired power plant, Energy Procedia, 37, 6248-6255.

Hirata, T., et al., 2014. Current status of MHI CO_2 capture plant technology, 500 TPD CCS demonstration of test results and reliable technologies applied to coal fired flue gas, to be presented in the 12nd International Conference on Greenhouse Gas Control Technologies (GHGT 12).

Jönssona, S., and Telikapalli, V.,2012. Chilled ammonia process installed at the Technology Center Mongstad, The 11st International Conference on Greenhouse Gas Control Technologies (GHGT-11), Kyoto, Japan, 18th-22nd November.

Just, P.-E.,2013. Advances in the development of CO2 capture solvents, *Energy Procedia*, **37**, 314-324.

Lombardo G., Agarwal R., Askander J.,2014. Chilled ammonia process at Technology Center Mongstad-first results, Energy Procedia, 51, 31-39.

Petra Nova Carbon Capture Project, 2014. http://www.globalccsinstitute.com/project/petra-nova-carbon-capture-project.

Reddy, S., Scherffius, J. R., Yonkoski, J., Radgen, P., and Rode, H.,2013. Initial results from Fluor's CO_2 capture demonstration plant using Econamine FG Plus^{SM} technology at E.ON Kraftwerke's Wilhelmshaven power plant, Energy Procedia, 37, 6216-6225.

3 Introduction

PCC is one of the leading capture technologies for significant reduction of CO_2 emission from coal fired power stations. Currently, the state of the art PCC technology is based on amine solutions, MEA in particular. A report by US Department of Energy (Ramezan, 2007) shows that the advanced amine technology will reduce the power plant efficiency by 30% and involve significant capital investment costs for retrofitting an existing coal fired power station (Conesville unit 5 in Ohio, subcritical, 90% capture). The incremental levelized cost of electricity (LCOE) is estimated to USD $69/MWh. Recent studies of low CO_2 emission technologies for power generation in the Australian context (EPRI, 2010) show that addition of an advanced amine PCC process (state of the art) and CO_2 transport and storage to a new coal fired power station (pulverised black coal, supercritical, 750 MW sent out) will lead to a decrease in plant efficiency from 38% to 28.4 % (25.3% decrease) and an increase in LCOE from $77 AUD/MWh to $167 AUD/MWh (Figure 1 a). As shown in Figure 1b, the significant increase is due to increase in capital (plant cost), fuel, O&M and CO_2 transport and storage. The capital cost increase accounts for almost 60% of the total incremental LCOE. High capital costs are due to the fact that the new plants have to process more than 33% of coal extra to have the same power output and need to remove a large amount of CO_2 from an even larger amount of flue gas and compress it. This involves an increase in the size of the existing equipment and introduction of flue gas desulfurization (FGD) unit and CO_2 capture and compression facilities.

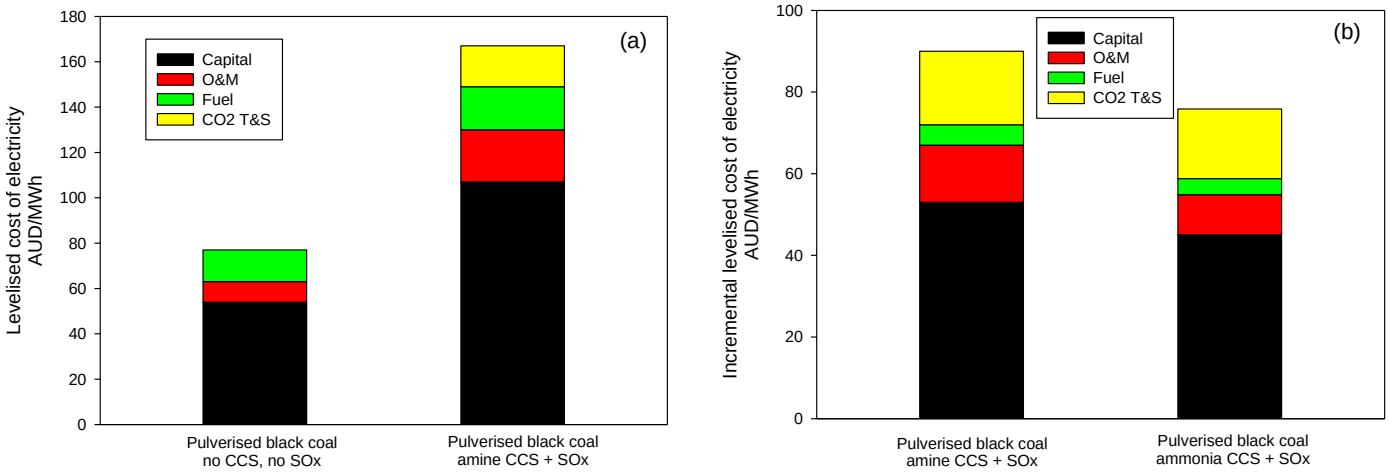

Figure 1 (a) Levelised cost of electricity (LCOE) for a new plant with and without CCS; (b) Incremental LCOE with the amine based CCS (The results are derived from (a)). The estimated incremental LCOE with the advanced ammonia based CCS is also included in (b) to demonstrate the potential benefits from using ammonia based CCS. The estimation is made in this work and based on assumption that the expected advancements for ammonia CCS can be achieved.

The advanced amine solvent has poor SO_X tolerance which requires a deep cut in SO_2 content to levels below 10 ppm. The cost of building a desulfurization unit is substantial. According to the EPRI report, in a

new plant in Australia in which the bare erected capital cost increase due to CO_2 removal and compression is $888 M AUD while capital increase due to clean up costs (installation of FGD) is $90 M AUD (EPRI, 2010). FGD alone will count for more than 9% of the increased capital costs.

It is clear that to make CCS technologies, and in particular PCC, economically more feasible, the research focus will be on the reduction of capital costs by using more efficient, smaller and cheaper units and development of solvents which require low parasitic energy consumption. The low energy consumption means the use of less coal and treatment of less gas, which results in a smaller facility, and has less environmental and health effects. In this context, the current submission is proposed, aiming at the development of advanced aqueous ammonia based PCC to achieve a significant cost reduction and reduce environmental risks.

Advantages of aqueous ammonia based PCC

Aqueous ammonia is a promising emerging solvent for CO_2 capture. Compared to other amines, ammonia, as one of the most widely produced chemicals in the world, is a low cost solvent, does not degrade in the presence of O_2 and other species present in the flue gas, and is less corrosive. The environmental and health effects of ammonia are well studied and are more benign than amines. Ammonia has a high CO_2 removal capacity and a low regeneration energy. It also has the potential of capturing multiple components (NO_x, SO_x, CO_2 and Hg) (Ciferno, 2005) and producing value added products such as ammonium sulphate and ammonium nitrate, which are widely used as fertilisers. This potential is of particular interest to Australian power stations since desulfurization and DeNOx are not implemented in Australia. It has been estimated by Powerspan (McLarnon, 2009) that the power plant efficiency loss is below 20% for an ammonia based capture process. A scoping study by US Department of Energy (Ciferno, 2005) suggested that the incremental cost of electricity using ammonia is less than half of that using traditional amines. It has to be pointed out that these reports assumed the availability of low temperature cooling water for solvent and flue gas cooling and recovery of ammonia. In Australia where ambient temperature is generally high, the energy consumption for production of low temperature cooling water is expected to be high, thus partially offsetting the energy saving from the solvent regeneration.

CSIRO has identified the aqueous ammonia based technology as a promising low cost technology for significant reduction of multiple components emissions from coal fired power stations in Australia. CSIRO and Delta Electricity completed pilot plant trials of the aqueous ammonia based capture technology under the real flue gas conditions in $7 M AUD pilot plant scale research facility at Delta's Munmorah Power Station in 2010. The pilot plant trials have confirmed the benefits and technical feasibility of the process and its potential for application in the Australian power sector. The benefits include high CO_2 removal efficiency (more than 85%) and production of high purity of CO_2 (99-100 vol%), and effectiveness of the combined SO_2 removal (more than 95%) and ammonia recovery, high stability of ammonia solvent and low regeneration energy. Part of the results were published in a number of conferences and journal papers (Yu, 2011a and 2011b). It is the first time that results from an actual aqueous ammonia plant operating on real flue gases have been published.

Areas for improvement

The pilot plant trials have identified a number of research opportunities to further develop aqueous ammonia based capture technologies.

- Relatively low CO_2 absorption rate compared to amine based solvent, which results in 2-3 times the number of absorbers compared to monoethanolamine (MEA, the benchmark solvent) and thus higher capital costs.
- Relatively high ammonia loss at high CO_2 absorption rate. The consumption of wash water is high.
- Operating the desorption process in a similar pattern to regular amine processes will result in the formation of ammonium-bicarbonate solids in the condenser, resulting in blockage.
- The available process simulation models were insufficient to support the process optimisation and scale up.

This limits the economical feasibility of the aqueous ammonia based PCC process. In this research project, CSIRO will collaborate with the University of Newcastle and Curtin University of Technology (by way of student exchange or other collaboration), exploring and evaluating novel approaches and concepts to further advance the aqueous ammonia based PCC process in Australian context.

References

Ciferno J., Philip D., Thomas T., 2005. An economic scoping study for CO_2 capture using aqueous ammonia. Final Report - DOE/NETL.

EPRI, 2010. Australian electricity generation technology costs-reference case 2010.

McLarnon C.R., Duncan J.L., 2009. Testing of ammonia based CO_2 capture with multi-pollutant control technology, Energy Procedia, 1, 1027-1034.

Ramezan M., Skone T.J., Nsakala N.Y., Liljedahl G.N, 2007. Carbon dioxide capture from existing coal-fired power plants, DOE/NETL-401/110907.

Yu H., Morgan S., Allport A., Do T., Cottrell A., McGregor J., Wardhaugh L., Feron P., 2011a. Results from trialling aqueous ammonia based post combustion capture in a pilot plant at Munmorah Power Station: Absorption, Chemical Engineering Research and Design, 89, 1204-1215.

Yu H., Morgan S., Allport A., Do T., Cottrell A., McGregor J., Feron P., 2011b. Results from trialling aqueous ammonia based post combustion capture in a pilot plant at Munmorah Power Station, Energy Procedia, V 4, 1294-1302, 10th International Conference on Greenhouse Gas Control Technologies.

4 Scope of the Project

This research project will further develop a promising aqueous ammonia (NH_3) based post combustion capture (PCC) process to achieve a significant reduction of investment and running cost in the Australian context and reduce potential environmental risks resulting from the implementation of PCC technologies.

The objectives of the project are:

1. Develop a novel aqueous ammonia based solvent which has fast CO_2 absorption rate equivalent to MEA while maintaining a low regeneration energy requirement.
2. Further advance the combined SO_2 removal and ammonia recovery technology to eliminate additional FGD, reduce the ammonia slip in the exiting flue gas to acceptable levels and produce a value added fertiliser, i.e. ammonium sulphate.
3. Further develop CSIRO technology (patent application no WO/2010/020017) to enhance CO_2 absorption, reduce ammonia loss and cooling water consumption.
4. Develop and validate a rigorous rate based model for the capture process which will guide process modification to achieve further savings on capture costs.

The research proposed here is to extend a number of novel approaches developed previously by CSIRO to address the issues identified, achieve the project objectives and thus make the process economically favourable. The new ideas and approaches include;

Promotion of CO_2 absorption rate through addition of promoters. Ammonia has been confirmed as a high loading capacity solvent and has a theoretically 1:1 ratio with CO_2 on a molar basis. It has been reported in a study by DOE (Ciferno, 2005) that the CO_2 carrying capacity in g CO_2 per g of ammonia solution (8 wt.%) circulated is 0.07 as compared with 0.036 g CO_2 per g MEA solution (20 wt.%). However, the CO_2 absorption rate is much lower in ammonia than in MEA, as identified by our recent pilot plant investigation (Yu, 2011a). This is preventing ammonia of achieving its high loading capacity and low regeneration energy potential.

The CO_2 absorption flux within the column can be correlated by $N_{CO2}= K_GA(P_{CO2}-P^*_{CO2})$, where N_{CO2} is CO_2 absorption flux, K_G mass transfer coefficient, P_{CO2} partial pressure of CO_2 in the flue gas, P^*_{CO2} CO_2 equilibrium partial pressure in the solvent and A, effective interfacial surface area. For a given CO_2 absorption flux to achieve a typically 85-90% CO_2 removal efficiency, K_G and ($P_{CO2}-P^*_{CO2}$), need to be high in order to reduce A, which is directly related to the size of column (capital cost).

Recent studies by CSIRO showed that with introduction of a small amount of additive such as an amino acid salt which is stable and cheap, the CO_2 mass transfer coefficients increase significantly (Yu, 2012). With the introduction of 0.3 M additive to 3 M ammonia, the mass transfer coefficients increase dramatically compared to ammonia alone. They are comparable with MEA at high CO_2 loadings which are relevant to industrial applications. It is expected that further tests of new additives and optimisation of the solvent will lead to the development of the novel ammonia based solvent with high mass transfer coefficients which match and are even higher than those for MEA while maintaining its low regeneration energy.

The promotion of CO_2 absorption in ammonia is relatively new and the mechanism involved is unknown. Recently CSIRO has developed a new software tool in Matlab® to model CO_2 absorption into aqueous MEA, PZ, ammonia and binary mixtures of PZ with AMP or ammonia (Puxty, 2011). The tool solves partial differential and simultaneous equations describing diffusion and chemical reaction automatically derived from reactions written using chemical notation. It has been demonstrated that by using reactions that are chemically plausible the mass transfer in binary mixtures can be described by combining the chemical reactions and their associated parameters determined for single amines. The observed enhanced mass transfer in binary mixtures can be explained through chemical interactions occurring in the mixture without need to resort to using additional reactions or unusual transport phenomena (e.g. the shuttle mechanism). Such a tool in conjunction with a stopped flow reactor at the University of Newcastle will help elucidate the promotion mechanism (Wang, 2011).

Combined removal of SO_2 and recovery of ammonia. This research project also tests a hypothesis that an integrated approach can be used to achieve the combined removal of SO_2 and recovery of ammonia. In this approach, as described in our publication (Yu, 2011a), the wash water is circulated between the pre-treatment column (before absorber) and wash column (after absorber). Ammonia recovered from the flue gas in the wash column is used to capture SO_2 in the pre-treatment column. The results from the pilot plant trials have demonstrated the effectiveness of the approach. More than 95% SO_2 in the flue gas and more than 80% ammonia which slips to flue gas in the absorber can be removed from the gas phase by the wash water. The removal of SO_2 from flue gas by ammonia is the established technology and its fundamentals have been well documented (Kohl and Nielsen, 1997). Ammonia has a strong affinity for SO_2, thus permitting a compact absorber with a very low liquid-to-gas ratio. The high-purity, high-market value ammonium sulphate crystals were successfully compacted into a premium granular by-product (Saleem, 1993). The combined removal of SO_2 and ammonia has a potential of reducing or offsetting the cost involved for removal of SO_2 and ammonia with production of saleable ammonium sulphate. The focus of the research project is to identify conditions under which SO_2 and ammonia are selectively removed at high efficiencies in preference to CO_2, understand the mechanism involved for oxidation of sulphite to sulphate, and explore more efficient methods for separation of ammonium sulphate from the aqueous ammonia solvent.

Absorption under pressure. This research project will also further develop a new concept developed by CSIRO. The flue gas is pressurised and absorption of CO_2, SO_2 and recovery of ammonia can take place under pressure. The flue gas cooling requirement is provided by the expansion of the flue gas after pressurisation. It is well known that pressurisation of flue gas will lead to high energy penalties but the size of absorption columns and ammonia loss as well as energy consumption for production of cooling water can be reduced significantly. In the Australian context, capital costs are the major contributors to the capture costs while fuel contribution is relatively small. The proposed high pressure absorption experiments and the rigorous process model to be developed will allow an evaluation of the feasibility of the concept and its economic viability.

Development of rate based absorption model. The available process simulation models were insufficient to support the process optimisation and scale up. The project will develop a rigorous rate based model for the advanced aqueous ammonia based capture process and validate the model with results from previous pilot plant trials and from experiments with the CSIRO's processes development facility. The developed model will be used to evaluate novel process concepts such as rich solvent recycle in the absorber and identify approaches to further reduce ammonia loss and energy and water consumption.

The research plan has been developed to carry out the proposed research activities. The project is planned over three year and divided into 6 stages with each stage being approximately 6 months. This report includes the results from the following research activities in Stage 4:

(1) Development and valiation of a rate based model for the system of NH_3-CO_2-SO_2-H_2O using Aspen Plus.
(2) Process modelling of a combined SO_2 removal and NH_3 recycle process. SO_2 and NH_3 absorption experiments on a bubble column were carried out to qualitatively confirm the modelling results.
(3) Development of ammonia based solvents which can match the standard MEA based solvents in terms of CO_2 absorption rate.
(4) Modelling of CO_2 absorption in piperazine promoted NH_3 solutions in a wetted wall column. This is the extenion of the work on the elucidation of promotion mechanism reported in the last progress report.

References

Ciferno J., Philip D., Thomas T., 2005. An economic scoping study for CO_2 capture using aqueous ammonia. Final Report - DOE/NETL.

EPRI, 2010. Australian Electricity Generation Technology Costs-Reference Case 2010.

Kohl. A. L, Nielsen R. B., 1997. Gas purification, 5th Ed, Gulf Professional Publishing.

Puxty G., Rowland R., Attalla M., 2011. Describing CO_2 mass transfer in amine/ammonia mixtures — No shuttle mechanism required, Energy Procedia, 4, 1369-1376.

Saleem, A., Janssen, K. E., Ireland, P. A., 1993. Ammonia scrubbing of SO_2 comes of age with In situ forced oxidation, paper presented at the EPRI/EPA/DOE 1993 SO_2 Control Symposium, Boston, MA, Aug. 24-26

Wang X.G., Conway W., Fernandes D., Lawrance G., Burns R., Puxty G., and Maeder M., 2011. Kinetics of the reversible reaction of CO_2(aq) with ammonia in aqueous solution. Journal of Physical Chemistry, A. 115, 6405–6412.

Yu H., Morgan S., Allport A., Do T., Cottrell A., McGregor J., Wardhaugh L., Feron P., 2011a. Results from trialling aqueous ammonia based post combustion capture in a pilot plant at Munmorah Power Station: Absorption, Chemical Engineering Research and Design, 89, 1204-1215.

Yu H., Morgan S., Allport A., Do T., Cottrell A., McGregor J., Feron P., 2011b. Results from trialling aqueous ammonia based post combustion capture in a pilot plant at Munmorah Power Station, Energy Procedia, V 4, 1294-1302, 10th International Conference on Greenhouse Gas Control Technologies.

Yu H, Xiang Q, Fang M, Qi Y and Feron P., 2012. Promoted CO_2 absorption in aqueous ammonia. Greenhouse Gases: Science and Technology 2, 1-9.

5 Approaches and Methodologies

This section describes the approaches and methodologies used for the following research activities:

(a) Development and validation of a rate-based model for the system of NH_3-CO_2-SO_2-H_2O using Aspen Plus

(b) Process modelling of a combined SO_2 removal and NH_3 recycle process using the developed rate-based model

(c) SO_2 and NH_3 absorption experiments on a bubble column to qualitatively validate the modelling results

(d) Modelling of CO_2 absorption in piperazine/ammonia mixture in a wetted wall column

5.1 Development of a rate-based model for the system of NH_3-CO_2-SO_2-H_2O

The rigorous rate-based process model is built within the RateFrac module in Aspen plus. The process model consists of a thermodynamic model, a transport model and a rate- based model. Thermodynamic model must be able to describe accurately the chemical equilibrium, vapour–liquid equilibrium, speciation and many other chemical and physical properties. The reliable transport model is required to calculate the density, viscosity, thermal conductivity, diffusion coefficient and surface tension of the electrolyte ammonia solvent.The rate-based model needs to completely characterise the material and energy balance, chemical kinetics, mass and heat transfer, hydrodynamics and column properties of the whole absorption and desorption system.

5.1.1 Thermodynamic and transport model

The Pitzer property method embedded in Aspen Plus is employed to calculate the chemical physical properties of the liquid phase including the fugacity coefficient, entropy, enthalpy and Gibbs energy, while the Redlich-Kwong-Soave equation of state is used to calculate the vapor phase fugacity coefficient. NH_3, CO_2, SO_2, N_2 and O_2 were defined as Henry components and the Henry's law constants of these species were retrieved from Electrolytes Expert System in Aspen plus. The Pitzer parameters for the binary interactions in the NH_3-CO_2-H_2O system are regressed against the literature experimental data of vapor-liquid equilibrium, heat capacity, ion speciation, which are automatically retrieved from the Aspen Plus databank (Aspen Technology, 2010a and 2010b).

The electrolyte solution characteristics and the liquid-vapor behaviors of the NH_3-CO_2-SO_2-H_2O system were modeled with an equilibrium chemistry package. Table 2 list all the reactions included in the package and their corresponding equilibrium constants. The chemical equilibrium constants of these reactions are expressed as:

$$\ln K_{eq} = A + B/T + C\ln(T) + DT$$

where K_{eq} is the equilibrium constant of each reaction; T is the temperature, K; constants A, B, C, D were adjustable parameters. The parameters for reactions 1-10 are available in the Aspen databank (Aspen Technology, 2010b) and those for the reaction $2HSO_3^-$ <--> $S_2O_5^{2-}$ + H_2O were obtained from Ermatchkov et al. (2005).

Table 2 Chemical reactions and equilibrium constants in the NH_3–CO_2–SO_2–H_2O system

No.	Reactions	Equilibrium parameter			
		A	B	C	D
1	$2H_2O$ <--> $H_3O^+ + OH^-$	132.899	-13445.9	-22.4773	0
2	$CO_2 + 2H_2O$ <--> $H_3O^+ + HCO_3^-$	231.465439	-12092.1	-36.7816	0
3	$HCO_3^- + H_2O$ <--> $CO_3^{2-} + H_3O^+$	216.049	-12431.7	-35.4819	0
4	$NH_3 + H_2O$ <--> $NH_4^+ + OH^-$	-1.2566	-3335.7	1.4971	-0.0370566
5	$NH_3 + HCO_3^-$ <--> $NH_2COO^- + H_2O$	-4.583437	2900	0	0
6	$2H_2O + SO_2$ <--> $H_3O^+ + HSO_3^-$	-5.978673	637.395996	0	-0.0151337
7	$H_2O + HSO_3^-$ <--> $H_3O^+ + SO_3^{2-}$	-25.290564	1333.40002	0	0
8	$2HSO_3^-$ <--> $S_2O_5^{2-} + H_2O$	-10.226	2123.6	0	0
9	NH_4HCO_3(S) <--> $NH_4^+ + HCO_3^-$	554.8181	-22442.53	-89.00642	0.06473205
10	$(NH_4)_2SO_3$(S) <--> 2 $NH_4^+ + SO_3^{2-}$	920.3782	-44503.83	-139.3449	0.03619046
11	$(NH_4)_2SO_3 \cdot H_2O$ (S)<--> 2 $NH_4^+ + SO_3^{2-} + H_2O$	-1297.041	33465.89	224.2223	-0.3515832

Transport properties are required when describing mass and heat transfer in the rate-based model for aqueous ammonia-based CO_2 capture. Various transport property models and corrections are embedded in Aspen Plus, and can be applied to calculate the density, viscosity, thermal conductivity, diffusion coefficient and surface tension of the NH_3–CO_2–SO_2-H_2O system. In this work, the liquid density of the electrolyte solutions is calculated using the Clarke model. The liquid viscosity is computed by the Andrade and DIPPR (Design Institute for Physical Properties) models and an electrolyte correction is applied using the Jones-Dole model. The surface tension of the aqueous ammonia solvent is calculated by the Hakim–Steinberg–Stiel and DIPPR models and corrected with the Onsager–Samaras model. The thermal conductivity is calculated by the Sato–Riedel and DIPPR models and the Vredeveld mixing rule, and adjusted using the Riedel model. The diffusivity of each species is determined using the Wilke–Chang model for molecular species and the Nernst–Hartley model for ions.

5.1.2 Rated-base model

The rate-based model embedded in the Aspen Plus RadFrac module is used to model CO_2 and SO_2 absorption in aqueous ammonia. The rate-based model can completely characterise the material and energy balance, chemical kinetics, mass and heat transfer, hydrodynamics and column properties of the absorption and desorption system.

The module allows users to divide the column into a number of stages along the column and perform material and energy balances at each stage, and integrate across the entire column. The model adopts the two-film theory and considers mass and heat transfer resistance in the liquid and gas phase (Whitman, 1923). The liquid film at each stage is discretised into several segments, as shown in Figure 2.

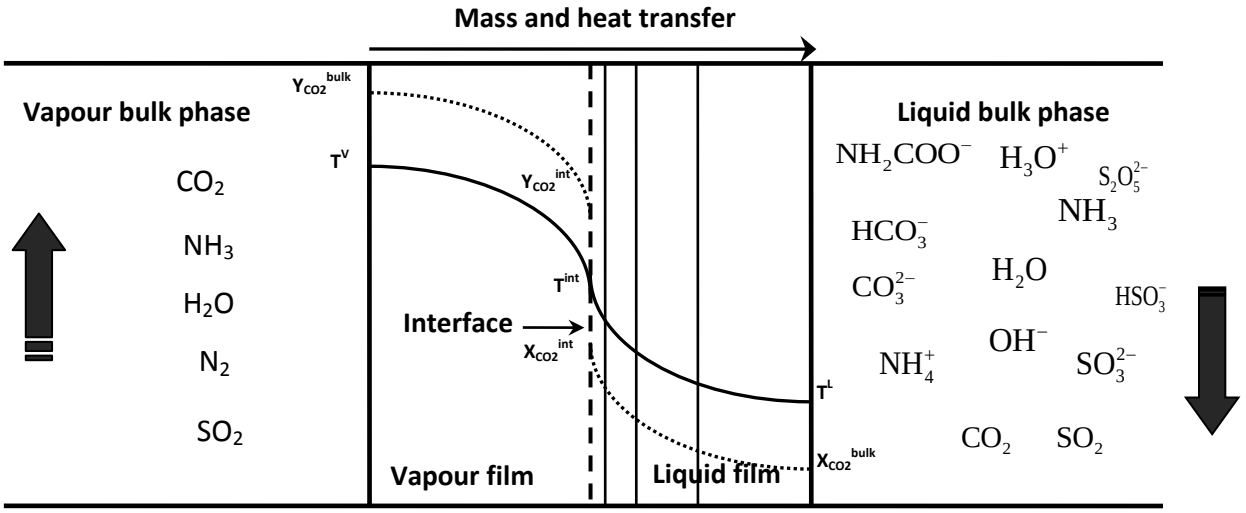

Figure 2 Schematic of discretised two-film model for the rate-based model in each stage

The segments near the interface are thinner than those close to the liquid bulk phase. This non-homogeneous discretisation allows more accurate calculation of species concentration profiles in the film. In this work, the film discretisation option is set to geometric sequence, the film discretisation ratio (ratio of film thickness of adjacent discretisation segments from bulk to interface) is set at 2, and the number of discretisation segments is 4. Combining the film equations with the material and heat balance equations at each stage allows the performance of the entire absorber/desorber column to be calculated. The rate-based model uses the Maxwell–Stefan theory to solve multi-component mass and heat transfer (Alopaeus, 1999).

For the calculation of mass and heat transfer, the rate-based model provides several built-in correlations to compute the gas and liquid mass and heat transfer coefficients for different packing types. Three mass transfer correlations developed by Onda et al. (1968), Billet and Schultes (1999) and Bravo and Fair (1985) can be selected. In this work, we chose the correlation proposed by Onda et al. (1968) to calculate the mass transfer properties for the random ring packing used in the Munmorah pilot plant. The Chilton–Colburn correlation is used to calculate the heat transfer in the absorber (Chilton et al. 1934).

The effective interfacial area is a critical parameter for both mass and heat transfer in the rate-based model. Yu et al. (2011) measured the effective interfacial areas as a function of the liquid flow rate for the packing used in the Munmorah pilot plant under typical operational conditions. Correlations from both Onda et al. (1999) and Billet and Schultes (1985) underpredict the effective interfacial area by approximately 20% and 40%, respectively, compared with the experimental results in the pilot plant. It is not clear why there are large discrepancies between the model prediction and the measurements. All correlations are empirically obtained and subject to the experimental conditions, packing materials used and the way how the materials are packed in the column. The pilot plant conditions are not exactly the same as those used for determination of the correlations. It is also possible that some pilot plant specific issues are responsible. But we were not able to determine which particular factor contributes most in the pilot plant campaigns. So we adopt a realistic approach: select the correlation from Onda et al. and set the interfacial area factor as a scaling factor for the effective interfacial area in the rate-based model at 1.2 to match the pilot plant measurements.

Four different flow models can be used to evaluate the liquid bulk properties: mixed, countercurrent, VPlug and VPlug-Pavg models. We chose the countercurrent model for this work, because it is suitable for

random packing columns (Chen, 2007). The countercurrent model determines the mass and heat transfer using the arithmetic average of gas and liquid phase bulk properties at the inlet and outlet of each stage.

Liquid holdup is used to calculate the kinetic reaction rate in the rate-based model. The correlation by Stichlmair et al. (1989) is applied to the holdup calculations. The liquid holdup value is set to 3% of the free volume under the reaction tab used for the model initialisation. The Tsai method is used to calculate pressure drop in the packed absorber (Tsai, 1985). The rate-based model uses the specific correlations for the mass transfer coefficients, interfacial area, liquid holdup and pressure drop to characterise the column hydrodynamics.

The chemical reactions model for the NH_3-CO_2-SO_2-H_2O system includes the equilibrium reactions listed in Table 2 and those kinetically controlled reactions listed in Table 3. We assume that reactions of CO_2 with OH^- and NH_3 are kinetically controlled. The power law expressions are used to express the kinetically-controlled reactions.

$$r = kT^n e^{-\frac{E}{RT}} \prod_{i=1}^{n} C_i^{a_i}$$

where r is the rate of reaction; k is the pre-exponential factor; n is the temperature exponent which is chosen as zero for this simulation; E is the activation energy; R is the universal gas constant; T is the absolute temperature; C_i is the molarity concentration of component i; a_i is the stoichiometric coefficient of component i in the reaction equation. The kinetic parameters k and E for kinetic reactions in Table 3 are derived from the work of Pinsent et al. (1956a and b).

Table 3 Kinetic parameters k and E for the reactions in the NH_3-CO_2-SO_2-H_2O system

No.	Reaction	Parameters	
		K	E(cal/mol)
1	$CO_2 + OH^- \rightarrow HCO_3^-$	4.32e+13	13249
2	$HCO_3^- \rightarrow CO_2 + OH^-$	2.38e+17	29451
3	$NH_3 + CO_2 + H_2O \rightarrow NH_2COO^- + H_3O^+$	1.35e+11	11585
4	$NH_2COO^- + H_3O^+ \rightarrow NH_3 + CO_2 + H_2O$	4.75e+20	16529

5.1.3 Pilot plant tests on Munmorah pilot plant

The results obtained from Munmorah pilot plant were used for model validation. In 2008 -2010, CSIRO in collaboration with Delta Electricity designed, constructed and operated a pilot plant at Munmorah Power Station and tested the aqueous ammonia based capture process under real flue gas conditions. The objectives were to address the gap in know-how on application of aqueous ammonia for post-combustion capture of CO_2 and to provide high quality pilot plant results for process model development and subsequent process optimisation and assessment.

Figure 1 shows the simplified flow-sheet of the Munmorah pilot plant, which consists of one pretreatment column, two absorber columns each with a separate wash column at the top, and one stripper. The pretreatment column works as a direct contact cooler for the flue gas and also serves as a scrubber for removal of SO_2 in the flue gas. The two absorbers provide flexibility in operation with different arrangements (single column or two columns in series or parallel). In case of series operation, the solvent

enters absorber 2 first and then absorber 1. The columns used in the pilot plant are constructed of stainless steel pipe (grade 304) and randomly packed with 16 or 25 mm Pall rings (Rhine Ruhr Pty Ltd.) which have the volumetric surface area of 340 or 207 m^2/m^3. The diameter of the columns, their packing heights and packing materials are listed in Table 4.

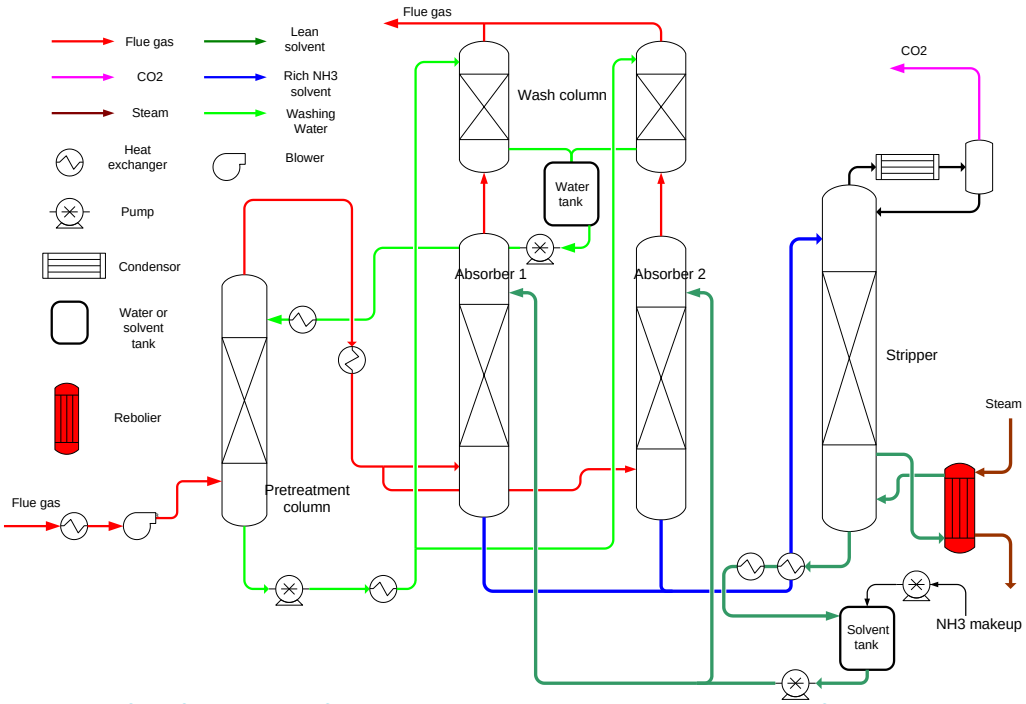

Figure 3 Simplified flowsheet of Munmorah pilot plant with operation of two columns in parallel

Table 4 Inner diameters of columns and packing heights

Columns	Diameter, mm	Packing height, m	Packing materials
Pretreatment column	500	3	25 mm Pall ring
Absorber[a]	600	2 or 3.9 (one column alone)	25 mm Pall ring
		5.8 or 7.8 (two columns in series)	
Wash column	500	1.8	25 mm Pall ring
Stripper	400	3.9	16 mm Pall ring

[a] The column packing heights can be varied which allows investigation of the effect of packing height on CO_2 removal.

Table 5 Typical inlet flue gas composition

CO_2	H_2O	O_2	NO	NO_2	SO_2	N_2
8.5-12 vol%	3-6 vol%	6.5-10 vol%	200-330 ppm	<10 ppm	190-280 ppm	76-78 vol%

Table 6 Summary of the experimental conditions

Parameter	Operational range
Ammonia concentration, wt%	0-6
CO_2 loading of lean solvent (mole CO_2/mole ammonia)	0-0.6
Wash water flow-rate, L/min	39
Liquid temperature in pretreatment and wash columns, ^oC	10-15
Solvent flow-rate, L/min	50-134
Gas flow-rate, kg/h	650-1000
Liquid temperature in absorber, ^oC	10-30
Gas pressure in absorber (absolute), kPa	101-150
Stripper bottom liquid temperature, ^oC	90-150
Stripper pressure (absolute), kPa	300-850

The detailed pilot trials have been described elsewhere (Yu, 2011 and 2012).

SO_2 removal experiments

Apart from CO_2 absorption and regeneration tests described above, an NH_3 dosing experiment was designed and carried out in the pilot plant to understand the characteristics of SO_2 removal by NH_3 and collect additional results for the model validation. The experiment was performed in the pretreatment column. The flue gas was introduced to the bottom of the column initially without liquid circulation. About 40 minutes after the introduction of flue gas, fresh water was introduced to the column from the top and circulated between the column and the wash water tank. The NH_3 was dosed into the wash water at different flow rates to investigate the effect of the NH_3 concentration in the solution on SO_2 removal. A Gasmet^{TM} analyzer (FTIR) (CX-4000) allowed online identification and quantification of gas species including CO_2, SO_2, NH_3 and H_2O in the flue gas at the inlet and outlet of the pretreatment column. pH of the solution at the outlet of the pretreatment column was measured online using an industrial pH meter (Rosemount). The detailed experimental activities and observations during the NH_3 dosing experiment are listed in Table 7.

Table 7 Experimental activities and observations in the SO_2 removal experiment. Flue gas flow-rate = 936 kg/h, CO_2 flow-rate = 120 kg/h, SO_2 concentration = ca. 200 ppmv, liquid flow-rate = 39 L/min, gas inlet temperature = 35-38 °C, inlet wash water temperature = 25°C

Stage	Time	Activities	pH	SO_2 removal	CO_2 removal	NH_3 outlet
1	9:04	Flue gas on	Not available	No	No	No
2	9:53	Water circulation	Drop to 2.5	Partial	No	No
3	11:40	Dosing NH_3 at 0.2 kg/h	Increase to 2.7	Partial	No	No
4	12:30	Dosing NH_3 at 0.5 kg/h	Increase to 7.2	Almost	No	No
5	13:33	Dosing NH_3 at 1 kg/h	Increase to 8.2	Complete	possible	Some
6	14:20	Dosing NH_3 at 1.8 kg/h	Increase to 8.6	Complete	possible	Sharp increase

5.2 Rate based modelling of combined SO_2 removal and NH_3 recovery

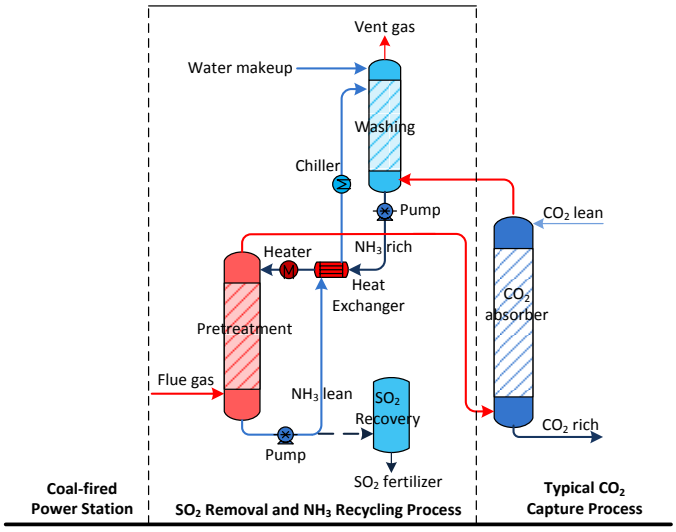

Figure 4 Combined SO_2 removal and NH_3 recycle process for CO_2 capture by aqueous ammonia

We proposed a novel process to combine capture of SO_2 and CO_2 using aqueous ammonia and reduce energy consumption for NH_3 recovery. Figure 4 shows the process flow-sheet diagram of the combined removal and NH_3 recycling system integrated with an aqueous ammonia based CO_2 capture unit (stripper is not shown). The whole system consists of a pretreatment column, an NH_3 wash column and a CO_2 absorber. Briefly, the vaporized NH_3 from CO_2 absorber was absorbed in the wash column. The NH_3-rich solution was collected at the bottom of the wash column and sent to the pretreatment column. In the pretreatment column, the hot flue gas directly contacted with the NH_3-rich solution. SO_2 was absorbed by the NH_3-rich solution and the captured NH_3 was desorbed by waste heat contained in the high temperature flue gas. The released NH_3 was recycled back to the CO_2 absorber as the make-up NH_3. The NH_3 lean solution was pumped to the top of the wash column for re-capturing the slipped NH_3. This was

one cycle. The solution was continuously circulated between the pretreatment column and wash column, and SO_2 was absorbed and accumulated in the SO_2-rich solution. After a number of circulations, the entire system reached a semi steady state when temperature in each stream remained constant while the concentrations of some species such as SO_2 increased. As shown in the analysis in the following section, the major species in the solution was $(NH_4)_2SO_3$ and its concentrations increaseed with circulation times. When the $(NH_4)_2SO_3$ concentration reached the saturation point, part of the solution will be transferred to the ammonium sulfate production unit. It should be mentioned that the fresh water was introduced into the wash column to maintain the water balance in the NH_3 recycle and SO_2 recovery system. A chiller was used to cool down the NH_3-lean solvent in order to achieve high NH_3 capture efficiencies, while a heater was used to heat up NH_3-lean solvent to further enhance NH_3 desorption and recycling.

We used the developed rate-based model to simulate the proposed process and assess its technical feasibility. The typical flue gas conditions from the power station and the CO_2 absorber are shown in Table 8 respectively. For the given flue gas conditions, the preliminary modelling of the process was carried out to determine a base case scenario under which the efficiencies of SO_2 removal and NH_3 recovery were high, the column sizes are small and there is no flooding in the columns . The conditions are as follows: 350 kg/hr wash water circulation rate; 10 °C wash water inlet temperature; wash column size $\emptyset\ (\text{inner diameter})0.5m \times h\ (\text{height})\ 3.0m$ with 16mm pall ring; pretreatment column size $\emptyset 0.5m \times h 3.0m$ with 25mm pall ring, 5°C temperature approach of the heat exchanger between the hot inlet and the cold outlet streams.

Table 8 The properties of the flue gas from power station and CO_2 absorber

Source	Flow-rate	Temperature	Composition, vol/%					
	Kg/hr	°C	CO_2	H_2O	O_2	N_2	NH_3	SO_2
Power station	760	120	10.7	6.0	7.8	75.5	-	200ppmv
CO_2 absorber	656	16.9	3.23	1.83	9.0	84.2	1.20	-

5.3 SO_2 and NH_3 absorption experiments

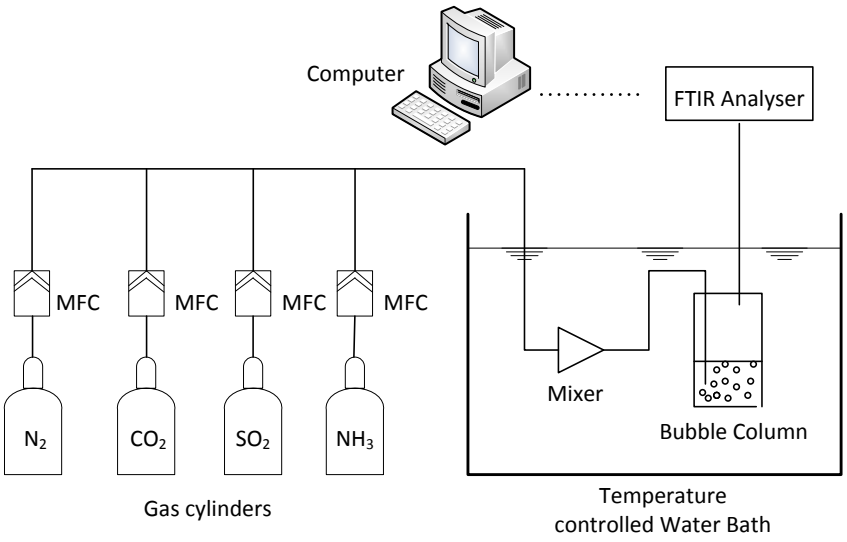

Figure 5 Schematic diagram of experimental apparatus

The SO_2 and NH_3 absorption experiments were carried out separately in a bubble column to help validate the simulation results. The schematic flow-sheet diagram of the experimental setups is shown in Figure 5. Carbon dioxide (99.8%), Nitrogen (99.9%), sulphur dioxide (1.0 % in N_2) and NH_3 (1.06 % in N_2) were used to produce the gas mixtures. The flow rates of the gases were controlled by mass flow controllers (Bronkhorst). The total gas flow rate was fixed at 5.0 L/min in the SO_2 removal experiments and 3.0 L/min in the NH_3 absorption experiments. The gases went through a mixer before entering the bubble column. Both the mixer and the bubble column were placed in the water bath to ensure that the gas temperature was close to the solvent temperature before the gas mixture entered the bubble column. The simulation results to be presented in the following section showed that the major species in the wash water is ammonium sulphite $(NH_4)_2SO_3$. Therefore the ammonium sulphite monohydrate ($(NH_4)_2SO_3 \cdot H_2O$, 92% purity from Sigma Aldrich) was used to prepare $(NH_4)_2SO_3$ solutions in the experiments to simulate the real process. The gas mixture was dispersed at the bottom of the bubble column and contacted the solvent with a short residence time. The FTIR gas analyzer (Gasmet™ Dx-4000) was used to determine the gaseous CO_2, SO_2, and NH_3 concentrations before and after absorption. The SO_2 and NH_3 removal efficiency can be expressed as the following equation. $\eta\% = \frac{c_{i,inlet} - c_{i,outlet}}{c_{i,inlet}} \times 100\%$ where η is the removal efficiency; i represents the component SO_2 or NH_3; $c_{i,inlet}$ is the inlet concentration of component i, ppmv; and $c_{i,outlet}$ is the outlet concentration of component i, ppmv. NH_3 removal efficiency is also called NH_3 reuse efficiency. The slipped NH_3 from the CO_2 absorber will go to three destinations: one is to be discharged into the atmosphere after the wash column (gas phase); the second is to be recycled to the CO_2 absorber (gas phase); and the third will be dissolved in the solution (liquid phase). The NH_3 in the second and third can be regarded as reuse (recycle).

In each experiment, 200 ml of solution was placed in the bubble column. During the absorption experiments, either SO_2 or NH_3 will build up in the solutions and the composition of the solution will change with time. As a result, the SO_2 and NH_3 removal efficiency will change accordingly. In this work, the

average value in the first one minute of the measurement was used. In this short period of time, the composition of the solution changed little.

5.4 Modelling of CO_2 absorption in piperzaine/NH_3 mixture in a wetted wall column

The availability of the detailed reaction scheme for the Piperazine (PZ)-NH_3-CO_2-H_2O system also makes it possible to rigorously simulate the mass transfer process in a gas –liquid contactor including the wetted wall column. The simulated results including CO_2 absorption flux or CO_2 mass transfer coefficients can be compared with experimental results to confirm the validity of the simulation and help identify and understand the factors which can influence the mass transfer. This exercise could help develop a rate based model for CO_2 absorption which can be used for process optimisation. The commonly used process simulation packages such as Aspen Plus requires thermodynamic, transport and rate-based models for the studied system in order to simulate the absorption process. However, for the new solvent system, these models are not available and the development of these models requires significant efforts. In this work, an in-house software tool implemented in the Matlab® was used to model the CO_2 mass transfer behavior in the NH_3 and PZ mixtures. The software tool solves partial differential equations and nonlinear simultaneous equations that define the diffusion, reaction and equilibrium processes occurring in a thin liquid film as a function of time and film depth (Puxty and Rowland, 2011). Axial dispersion and heating effects are neglected and the equations are solved in one dimension perpendicular to the gas-liquid interface. It is also assumed that physical properties such as viscosity and density remain invariant within the film.

In brief, the system of partial differential equations to be solved are defined as a combination of Fick's law (diffusion) and chemical reaction (Cussler, 2009; Danckwerts, 1970):

$$\frac{\partial C_i}{\partial t} = D_i \frac{\partial^2 C_i}{\partial x^2} - r_i$$

where D_i is the diffusion coefficient of species i ($m^2 \cdot s^{-1}$), c_i is the concentration of species i in molarity (M), x is the distance from the gas-liquid interface (m), t is time (s) and r_i is the rate of formation or destruction of i by chemical reaction ($M.s^{-1}$). The chemical model used was identical to that described the previous report. The Matlab® function pdepe, which relies on the method of lines, was used to numerically solve the complete system of partial differential equations assuming slab geometry. The pdepe function automatically determines the grid spacing in both time and space to achieve results of a specified accuracy. Once the solution of this equation has been calculated for a given gas-liquid exposure time (t_e) the time average CO_2 absorption flux can be calculated at the gas-liquid interface (x = 0) according to the following equation.

$$r_{CO_2}^{calc} = -A\frac{D_{CO_2}}{t_e}\int_0^{t_c}\frac{\partial C_{CO_2}}{\partial t}dt$$

Diffusion coefficients for CO_2 and all other species and the exposure time were calculated as previously described (Dubois and Thomas, 2011) based on the measured viscosity and density and the wetted-wall operating conditions. The concentration of CO_2 at the gas-liquid interface was calculated using the Henry constant from Crovetto et. al. (1991). The ρ is the density of the solutions.

$$H_{CO_2} = \frac{\exp(9.4052 + \frac{3934.40}{T} - \frac{941290.2}{T^2})}{\frac{\rho}{1801}}$$

The liquid side mass transfer coefficient, k_L, can be determined from the calculated results in the same manner as K_G is determined from the wetted-wall data. If the gas-side resistance to mass transfer is assumed negligible (which is the case for the 5 L.min^{-1} gas flow rate used) k_L (liquid phase mass transfer coefficient) ≈ K_G.

References

Alopaeus, V., Aittamaa J., Nordén, H.V. 1999. Approximate high flux corrections for multi- component mass transfer models and some explicit methods. Chemical Engineering Science, 54(19), 4267–4271.

Aspen Technology. 2010a. Aspen physical property system: physical property models. Burlington, MA, USA.

Aspen Technology. 2010b. Rate-based model of the CO_2 capture process by NH_3 using Aspen Plus. Burlington, MA, USA.

Billet, R., Schultes, M. 1999. Prediction of mass transfer columns with dumped and arranged packings: updated summary of the calculation method of billet and schultes. *Chemical Engineering Research and Design*, 77, 498–504.

Bravo, J. L., Rocha, J. A. and Fair, J. R. 1985. Mass transfer in gauze packing, Hydrocarbon Processing, 64(1): 91-95.

Chen E., 2007. A carbon dioxide absorption into piperazine promoted potassium carbonate using structured packing. Ph. D. thesis. The University of Texas at Austin, USA.

Chilton, T.H., Colburn, A.P. 1934. Mass transfer (absorption) coefficients prediction from data on heat transfer and fluid friction. Industrial & Engineering Chemistry, 26, 1183−1187.

Cussler, E.L. 2009. Diffusion Mass Transfer in Fluid Systems, 3rd ed. Cambridge University Press, Cambridge.

Danckwerts, P.V. 1970. Gas-Liquid Reactions. New York, McGraw-Hill.

Dubois, L., Thomas, D. 2011. Carbon dioxide absorption into aqueous amine based solvents: modeling and absorption tests. Energy Procedia 4, 1353-1360.

Crovetto, R. 1991. Evaluation of solubility data of the system CO_2-H_2O from 273-K to the critical-point of water. Journal of Physical Chemical Reference Data, 20, 575-589.

Ermatchkov, V., Kamps, A. P.S., Maurer, G., 2005. The chemical reaction equilibrium constant and standard molar enthalpy change for the reaction: $\{HSO_5^{2-}(aq) \rightleftarrows S_2O_5^{2-}(aq) + H_2O(l)\}$. a spectroscopic and calorimetric investigation, The Journal of Chemical Thermodynamics, 37, 187–199.

Onda, K., Takeuchi, H., Okumuto, Y., 1968. Mass transfer coefficients between gas and liquid phases in packed columns. Journal of Chemical Engineering of Japan, 1, 56–62.

Pinsent, B.R.W., Pearson, L., Roughton, F.J.W., 1956a. The kinetics of combination of carbon dioxide with hydroxide ions. Transactions of Faraday Society, 52, 1512−1520.

Pinsent, B.R.W., Pearson, L., Roughton, F.J.W., 1956b. The kinetics of combination of carbon dioxide with ammonia, Transactions of Faraday Society, 52, 1594-1598.

Puxty, G., Rowland, R., 2011. Modeling CO_2 mass transfer in amine mixtures: PZ-AMP and PZ-MDEA. Environmental Science & Technology 45, 2398-2405.

Stichlmair, J., Bravo, J.L., Fair, J.R., 1989. General model for prediction of pressure drop and capacity of countercurrent gas/liquid packed columns. Gas Separation & Purification, 3, 19–28.

Tsai, T.C., 1985. Packed tower program has special features, Oil and Gas Journal, 83, 77.

Yu, H., Morgan, S., Allport, A., Cottrell, A., Do, T., McGregor, J., Wardhaugh, L., Feron, P., 2011a. Results from trialing aqueous NH_3 based post-combustion capture in a pilot plant at Munmorah power station: Absorption. Chemical Engineering Research and Design, 89, 1204–1215.

Yu, H., Qi, G., Wang, S., Morgan, Allport, A., Cottrell, A., Do, T., McGregor, J., Wardhaugh, L., Feron, P., 2012. Results from trialing aqueous ammonia-based post-combustion capture in a pilot plant at Munmorah Power Station: Gas purity and solid precipitation in the stripper. International Journal of Greenhouse Gas Control, 10, 15–25.

Whitman, W.G., 1923. Preliminary experimental confirmation of the two-film theory of gas absorption. Chemical & Metallurgical Engineering, 29, 146–148

6 Results and Discussion

6.1 Validation of a rate-based model for the system of NH_3-CO_2-SO_2-H_2O using Aspen Plus

The validation of the thermodynamic model is one of the pre-requisites and foundation for the development of a rigorous rate-based model. We used the developed thermodynamic model of the NH_3-SO_2-CO_2-H_2O system to predict chemical and physical properties in ternary systems of NH_3-CO_2-H_2O (CO_2 capture process) and NH_3-SO_2-H_2O (SO_2 capture process) and quaternary system of NH_3-SO_2-CO_2-H_2O (combined CO_2/SO_2 removal and NH_3 recycling). The predicted results are compared with experimental date available in the literature.

6.1.1 Validation of thermodynamic model

(a) NH_3-CO_2-H_2O system

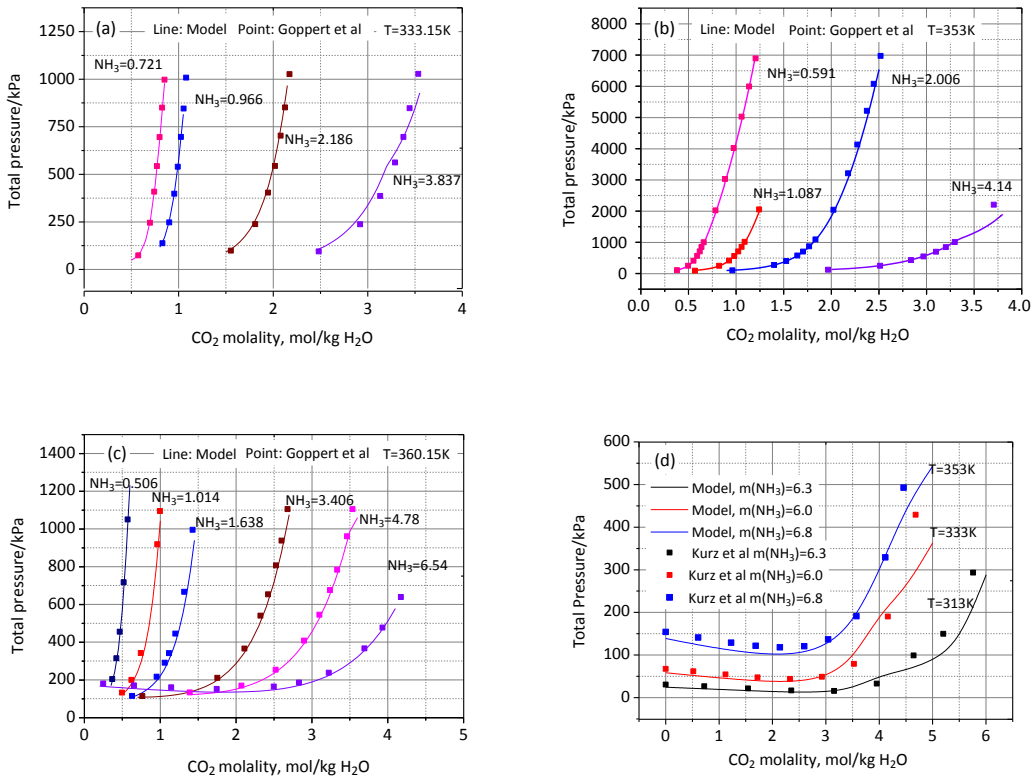

Figure 6 Comparison of experimental total pressure and predicted data as a function of CO_2 molality at various ammonia concentrations and temperatures. Experimental data (point) from GÖppert et al. (1988) and Kurz et al. (1995)

Figure 6 shows comparison of experimental total pressure and predicted data as a function of CO_2 molality at various ammonia concentrations and temperatures. Figure 7 shows comparison of experimental and predicted CO_2 partial pressure as a function of CO_2 molality at various ammonia concentrations and two temperatures, 333 K and 353 K. The experimental and predicted species profiles as a function of CO_2

molality at the ammonia concentration of 6.3 mol NH_3/kg H_2O and 313 K are presented in Figure 8. The good agreement between the experimental and modelling results are obtained.

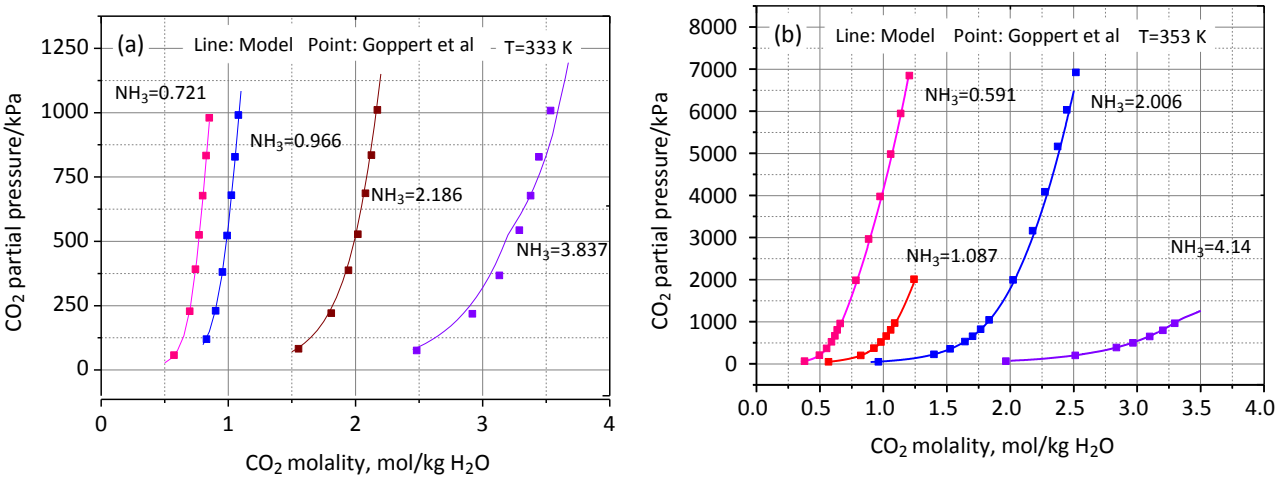

Figure 7 Comparison of experimental (point) and predicted (line) CO_2 partial pressure as a function of CO_2 molality at various NH_3 concentrations and (a) T=333K; (b) T=353 K. Experimental CO_2 partial pressure results are from GÖppert et al (1988).

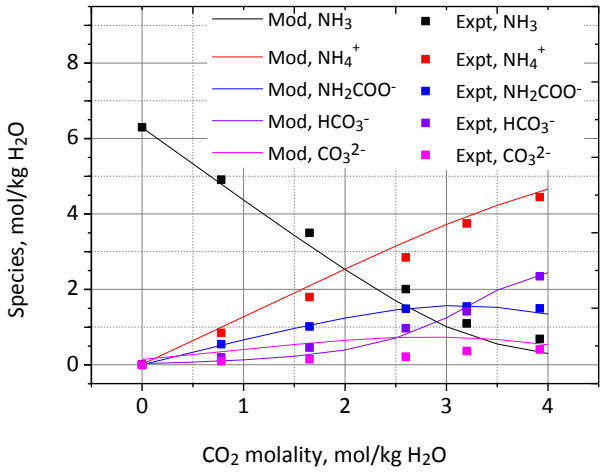

Figure 8 Comparison of experimental (point) and predicted (line) liquid species distribution as a function of CO_2 molality at the ammonia concentration of 6.3 mol/kg H_2O and 313 K. Experimental results are from Lichtfers [25]

(b) NH_3-SO_2-H_2O system

Figure 9 plots the modelled and experimental total pressures in the NH_3-SO_2-H_2O system as a function of SO_2 molality at two ammonia concentrations. The predicted total pressures agree reasonably well with the experimental measurements. Overestimation of the total pressure is observed at high SO_2 concentrations (above 6 mol/kg H_2O). This is likely due to the limitation of Pitzer model in which the electrolytes concentration in the solution should be no more than 6 mol/L (Aspen Technology, 2010). Another possibility of the deviations might be due to the uncertainty of measurements at high temperature and high loading. Considering that the proposed process was carried out in the electrolytes concentration

range of 0-6 mol/L and at temperatures below 353 K, the model is suitable for the prediction of vapor-liquid equilibrium.

.

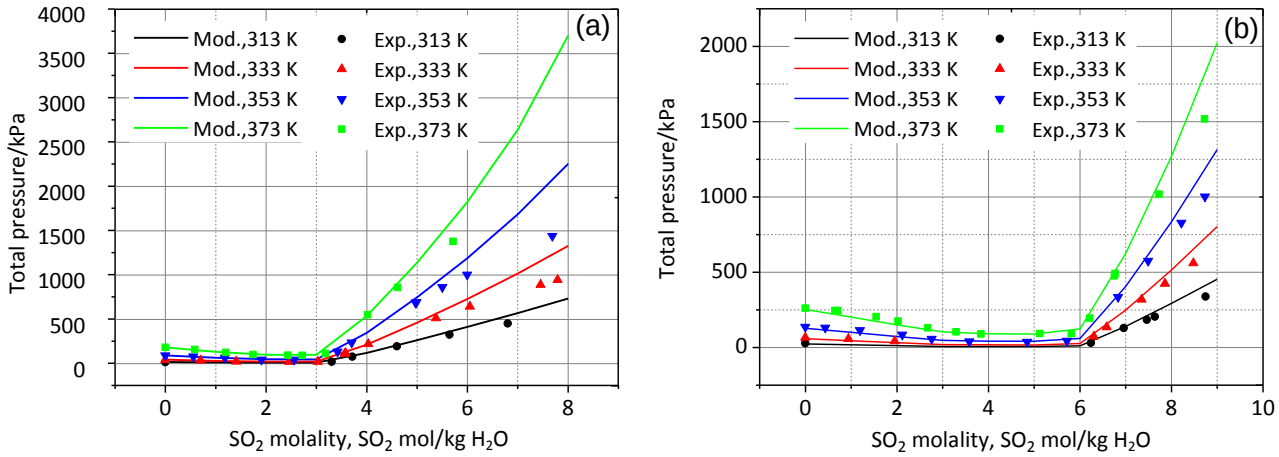

Figure 9 Total pressure of NH_3-SO_2-H_2O for different temperatures at (a) mNH_3=3.19 mol/kg H_2O , (b) mNH_3=6.08 mol/kg H_2O with model data and experiment data from Rumpf et al [26]

The solution pH can reflect the species distribution such as HSO_3^-, SO_3^{2-}, $S_2O_5^{2-}$. As shown in Figure 10, the modelled pH values agree well with the experimental results at the electrolytes concentrations ranging from 0.001 mol/L to 6 mol/L. This implies that the proposed thermodynamic model also has the capability to predict the ionic species concentration in the NH_3-SO_2-H_2O system.

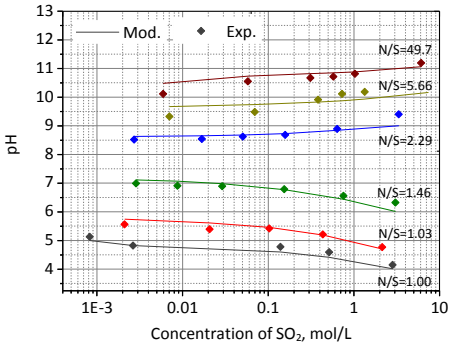

Figure 10 pH of solutions at a function of SO_2 concentrations at different NH_3/SO_2 (N/S) molar ratios and 293 K. Experimental data are obtained from Scott & McCarthy (1967)

(c) NH_3-CO_2-SO_2-H_2O

Figure 11 compares the predicted and experimental CO_2 partial pressure in the SO_2 loading range of 0-0.3 (mol SO_2/mol NH_3) and temperature range of 293-333 K. These conditions are relevant to the actual conditions of the combined SO_2 recovery and NH_3 recycling process. As shown in Figure 11, the model prediction agrees reasonably well with the experimental results, although a small deviation was observed at CO_2 molality over 0.5 mol/kg H_2O. Considering that the SO_2 removal and NH_3 recycling process will be carried out at low CO_2 concentrations (below 0.5 mol/kg H_2O), the effect of the deviation can be neglected.

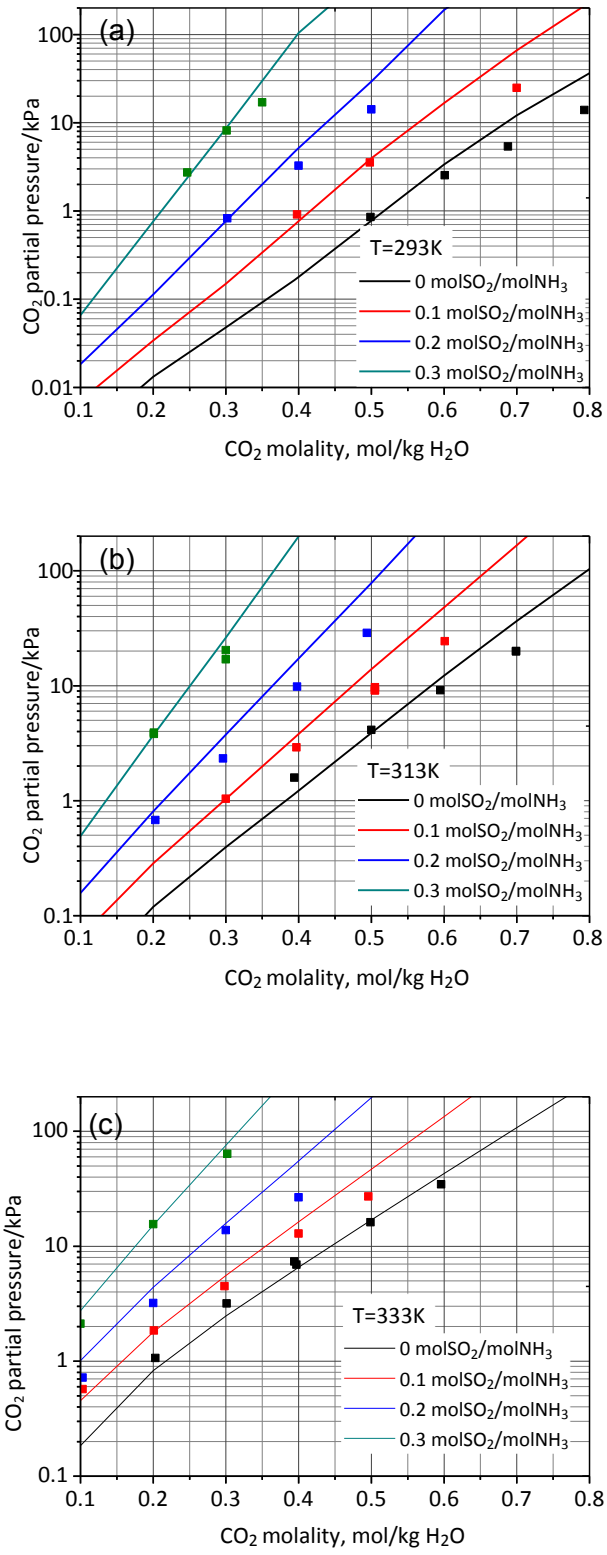

Figure 11 Predicted and measured CO_2 partial pressure of NH_3-CO_2-SO_2-H_2O system as a function of CO_2 molality at various SO_2 loadings (molar ratio of SO_2 to NH_3) and the ammonia concentration of 5 wt%. (a) 293 K, (b) 313 K and (c) 333 K. Experimental data are obtained from Qi (2014)

In summary, the developed thermodynamic model can satisfactorily predict the vapor-liquid equilibrium and ions speciation not only for the ternary systems, NH_3-CO_2-H_2O system and NH_3 -SO_2-H_2O system, but also for the quaternary NH_3-CO_2-SO_2-H_2O system.

6.1.2 Validation of the rate-based model

The rate-based model was validated using pilot plant results from CO_2 absorption, CO_2 regeneration and NH_3 dosing experiments respectively.

(a) CO_2 absorption in a packed column

Table 9 shows the comparison of pilot plant and predicted results under a variety of experimental conditions. As shown in Table 9, the average relative error for the overall CO_2 absorption rate in 30 tests is ±6.0%, and for NH_3 loss rate in 24 tests is ±11.1%. The comparison of the CO_2 absorption rate and ammonia loss rate between the modelling and experimental results are also presented in Figure 12. Generally good agreement between the experimental and modelling results was obtained.

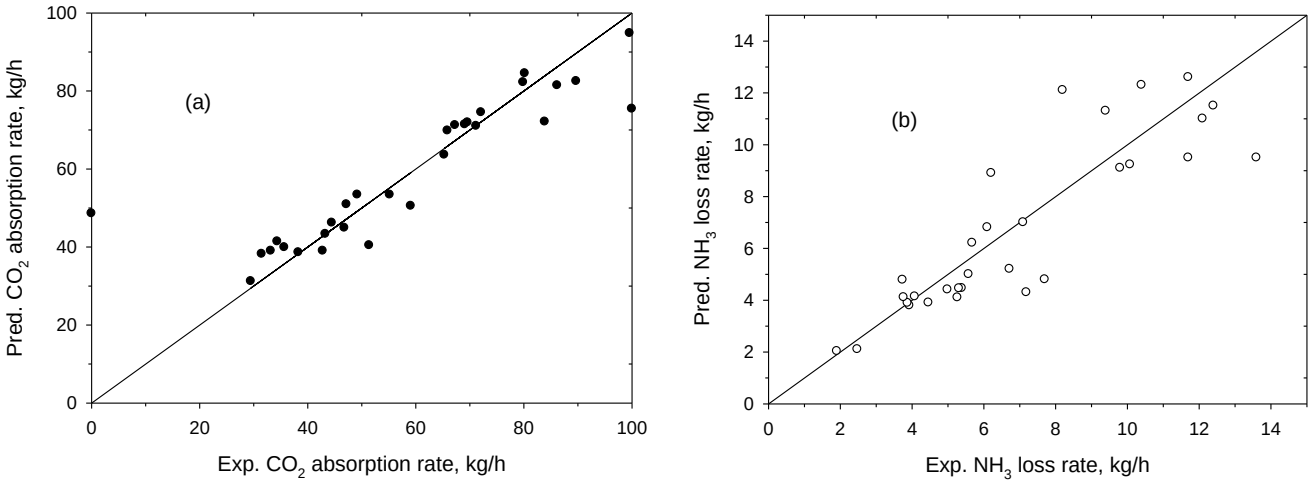

Figure 12 Comparison of (a) CO_2 absorption rate and (b) ammonia loss rate between pilot plant tests and rate-based model under the conditions listed in Table 9

.

Table 9 Summary of rate-based model predictions and pilot-plant trial results conducted under a variety of experimental conditions in absorber

Test ID	30	31	31R	31B	32	32A	32B	33	34	34R1	34R2	36	35B	35	39	38
Key test conditions [a]																
Solvent flow-rate, L/min	134	134	134	134	134	134	134	100	67	67	67	134	134	134	134	134
Liquid inlet Temperature, ^{o}C	23.9	27	32.3	16.4	25.8	16.8	17.0	15.5	15.2	15.5	15.6	14.5	19.9	16.4	16.3	17.1
NH_3 wt%	4.9	4.08	4.21	3.79	3.56	4.19	3.98	4.24	4.37	4.37	4.00	4.97	5.82	4.96	4.49	1.92
Lean CO_2 loading [c]	0.24	0.24	0.23	0.25	0.24	0.26	0.22	0.21	0.22	0.23	0.22	0.41	0.36	0.31	0.28	0.22
Flue gas flow-rate, kg/h	646	646	632	750	780	760	821	817	906	915	916	799	799	799	898	912
Flue gas inlet CO_2, vol%	8.6	9.4	9.8	7.6	8.8	10.8	8.1	8.0	10.1	9.4	9.4	9.8	9.4	8.0	10.1	11.7
Comparison of test results and simulation results																
Exp. CO_2 absorption rate [g](Absorber1),kg/h	32.2	59.1	55.2	38.3	44.5	49.2	46.8	51.4	34.4	33.2	31.5	29.5	35.7	42.8	47.2	43.3
Pred. CO_2 absorption rate(Absorber1), kg/h	48.6	50.5	53.4	38.6	46.2	53.4	44.9	40.4	41.4	39	38.2	31.2	39.9	39	50.9	43.3
Relative error	--	14.5%	3.3%	0.8%	3.8%	8.5%	4.0%	21.4%	20.3%	17.4%	21.2%	5.7%	11.7%	8.8%	7.8%	0%
Exp.overall CO_2 absorption rate [g], kg/h	66.6	79.6	77.7	68.2	75.9	87.8	80.5	85.9	78.3	74.4	70.0	60.4	70.6	81.2	85.6	74.9
Pred. Overall CO_2 absorption rate, kg/h	70.1	74.8	77.3	61.7	75	87.2	71.9	67.1	75.8	72.4	72.9	57.6	68.3	64.3	87.1	83.8
Relative error	5.2%	6.0%	0.5%	9.5%	1.1%	0.7%	10.6%	19.5%	3.2%	2.7%	2.8%	4.6%	3.2%	20.8%	1.7%	11.8%
Exp. NH_3 loss rate [g](Absorber1),kg/h	7.10	6.10	10.08	3.93	5.68	4.46	5.58	5.39	3.88	5.31	4.08	2.48	3.74	3.77	4.99	1.91
Pred. NH_3 loss rate (Absorber1),kg/h	7.00	6.81	9.23	3.79	6.21	3.9	5.00	4.46	3.89	4.45	4.14	2.10	4.78	4.11	4.41	2.03
Relative error	1.4%	11.6%	8.4%	3.6%	9.3%	12.6%	10.4%	17.3%	0.3%	16.2%	1.0%	15.3%	--	9.0%	11.6%	6.3%

Table 9 continued

Test ID	44-1	44-2	45	46	47	47 B	48	50	51	52	53	54	55	56
							Key test conditions							
Solvent flow-rate, L/min	67	67	67	67	67	67	67	50	50	100	50	67	67	67
Liquid inlet Temperature, ^{o}C	15.8	12.7	15.9	18.9	28.0	27.0	23.2	23.0	24.1	22.4	23.1	23.1	23.4	22.8
NH_3 wt%	3.30	4.40	4.04	3.95	4.53	3.83	4.56	4.77	4.22	4.33	4.08	4.84	4.62	4.41
Lean CO_2 loading [c]	0.22	0.24	0.21	0.22	0.23	0.14	0.22	0.17	0.18	0.22	0.18	0.19	0.18	0.22
Flue gas mass flow-rate, kg/h	795	774	641	638	667	665	1000	661	1003	1060	972	925	903	837
Gas temperature, ^{o}C	15-20	15-20	15-20	15-20	15-20	15-20	15-20	15-20	15-20	15-20	15-20	15-20	15-20	15-20
Inlet CO_2 flow-rate, kg/h	125.9	113.1	98.4	97.5	103.0	105.7	150.5	102.5	158.3	157	131.3	132.7	127	122
Inlet NH_3 flow-rate, kg/h	0.9	0.28	0.44	0.5	1.2	1.3	0.7	1.3	1.3	2.1	0.6	0.5	0.6	n.a
Inlet H_2O flow-rate, kg/h	6.8	5.3	4.6	4.4	6.0	6.7	7.2	6.8	8.8	6.6	6.5	6.6	n.a	n.a
							Comparison of test results and simulation results							
Exp. CO_2 absorption rate [g], kg/h	69.6	69.1	67.3	65.9	71.2	79.9	86.2	72.1	83.9	99.6	65.3	80.2[l]	89.7[l]	85
Pred. CO_2 absorption rate, kg/h	71.9	71.4	71.2	69.8	71.0	82.2	81.4	74.5	72.1	94.8	63.6	84.5	82.5	75.4
Relative error, %	3.3%	3.3%	5.8%	5.6%	0.3%	2.9%	5.7%	3.3%	14.1%	4.8%	2.6%	5.4%	8.0%	11.3%
Exp. NH_3 loss rate, kg/h	5.27	6.72	7.19	7.70	11.7	13.6	12.4	6.21	11.7	12.1	9.4	10.4	8.2	9.8
Pred. NH_3 loss rate, kg/h	4.1	5.2	4.3	4.8	9.5	9.5	11.5	8.9	12.6	11.0	11.3	12.3	12.1	9.1
Relative error, %	22.2%	22.6%	--	--	18.8%	--	7.2%	--	7.7%	9.1%	20.2%	18.2%	--	7.1%

Note: ‘a’: more details on test 30-38 in Qi (2013); ‘c’: defined as the molar ratio of total C-containing species to the total N-containing species (C/N molar ratio, mol/mol). ‘--‘: great error between test and simulation; ‘g’: CO_2 absorption rate based on gas analysis ; ‘l’: CO_2 absorption rate based on liquid analysis ; ‘n.a’: not

(b) CO_2 regeneration in a packed column

Table 10 lists pilot plant and predicted results obtained from solvent regeneration experiments under a variety of experimental conditions. In the process simulation, the Design Specs embedded in Aspen Plus were used. The variable parameters were condenser duty and reboiler duty; the design specifications were condenser temperature and the flow rate of CO_2 product. Aspen Plus automatically finds the accurate value of variable parameters to achieve design specifications during the simulation process.

Figure 13 shows the parity plot of energy requirement obtained experimentally and from the rate-based simulation in Aspen Plus. The energy consumption in pilot plant trials was calculated by two methods (Yu et al., 2012a), which are marked as Regeneration Energy (solvent) and Regeneration Energy (Steam) in Table 10 and Figure 13.

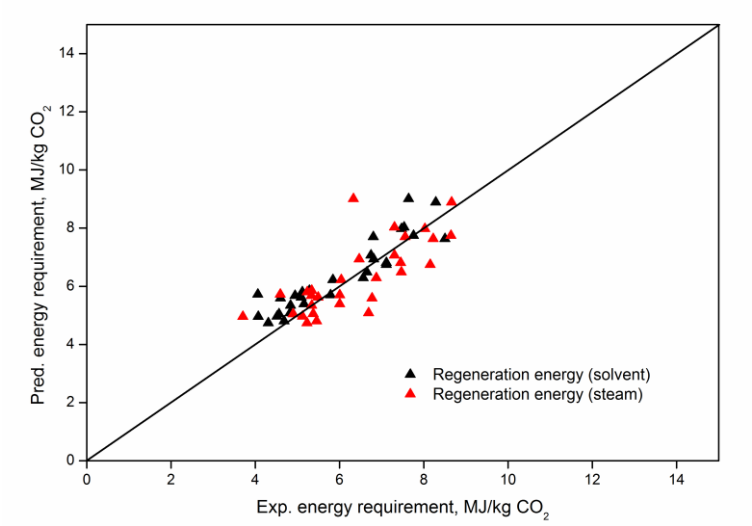

Figure 13 Parity plot of energy requirement obtained experimentally and predicted from the rate-based model under the conditions listed in Table 3

From the solvent side, the energy consumption can be calculated using the following equation:

$$Q_R = H_S + H_D - Q_C - Q_L$$

H_S represents the sensible heat required to heat the solvent from the stripper inlet temperature to the stripper outlet temperature (stripping temperature), and H_D is the energy required to desorb CO_2 from the solvent, which can be calculated by multiplying the heat of desorption by the CO_2 desorption rate. The CO_2 heat of desorption was estimated using Aspen Plus**.** Q_C is the heat duty of condenser, and Q_L stands for stripper heat loss, which can be estimated from the water-only experiments. From the steam side, energy consumption can be calculated directly from the steam consumption rate and latent heat of evaporation of water.

Good agreement has been achieved between the results. The relative deviations between the predicted and experimental results for most of the 30 cases considered are below 15%. Significant deviations are observed for several cases, which may be caused by discontinuous operation of the pilot plant, resulting from solid formation in the condenser and reflux lines (Yu et al., 2012b).

Table 10 Summary of rate-based model predictions and pilot-plant trial results conducted under a variety of experimental conditions in stripper

Test ID	30	31	31R	31B	32	32A	32B	33	34	34R1	34R2	36	35B	35	39
Key test conditions															
NH_3, wt%	4.9	4.08	4.21	3.79	3.56	4.19	3.93	4.24	4.37	4.37	4	4.97	5.82	4.96	4.49
Loading rich	0.3	0.32	0.32	0.33	0.37	0.36	0.32	0.34	0.37	0.4	0.39	0.46	0.43	0.39	0.38
Loading lean	0.24	0.24	0.23	0.25	0.24	0.26	0.22	0.21	0.22	0.23	0.22	0.41	0.36	0.31	0.28
Flow rate, L/min	134	134	134	134	134	134	134	100	67	67	67	134	134	134	134
P in stripper, kPa	600	600	600	600	600	600	600	600	600	400	600	600	600	600	450
CO_2 regeneration rate, kg/h	66.6	79.6	77.7	68.2	72.1	87.8	80.5	85.9	78.3	74.4	67.8	60.4	70.6	81.2	85.6
Condenser T, °C	26.1	28.5	27.6	21.9	25	27.7	26.4	25.5	25.4	23.5	25.3	23.4	23.4	26.2	22.4
Rich in T, °C	117.6	120.1	117.9	116.8	118.6	116	118.3	118.9	115.7	108.07	116.74	101.2	101.8	108.6	107.2
Comparison of test results and simulation results															
Exp., °C	129.2	131.6	129.1	129.8	129.7	128.5	131.6	132	130.2	119.63	131.97	111.5	113.6	121.1	118.9
Pred.,°C	127.9	130.6	130.2	130.4	128.2	128.6	131.8	131.9	130.1	118	130.7	114.3	114.9	120.1	117.3
Exp. average, ppm	n.a	n.a	n.a	446	523	1621	906	1421	1173	1135	998	374	625	658	1033
Pred., ppm	1569	1690	1563	733	955	1514	1283	1260	1196	1122	1094	899	1091	1386	1306
Exp. (solvent), kW	143.5	150.6	146.8	156.9	142.4	164.5	167.1	139.4	112.2	96.8	109	128.2	147.7	160.4	156.1
Exp. (steam), kW	159.9	143	163.1	164.1	163.3	178.2	179.4	144.1	130.6	112.8	113.1	106.2	143.3	168.1	163.4
Pred., kW	143.3	153.4	166.3	168.5	135.1	172.4	178.4	148.6	117.4	99.3	107.4	151.2	157.6	153.6	149.5

Table 10 continued

Test ID	37	38	44	44R	45	46	47	47B	50	48	51	52	53	54	55
							Key test conditions								
NH_3, wt%	4.14	1.92	3.3	4.4	4.04	3.95	4.53	3.83	4.77	4.56	4.22	4.33	4.08	4.84	4.62
Loading rich	0.44	0.4	0.39	0.37	0.35	0.36	0.38	0.33	0.36	0.38	0.41	0.36	0.39	0.35	0.38
Loading lean	0.35	0.22	0.22	0.24	0.21	0.22	0.23	0.14	0.17	0.22	0.18	0.22	0.18	0.19	0.18
Flow rate, L/min	134	134	67	67	67	67	67	67	50	67	50	100	50	67	67
P in stripper, kPa	600	600	400	400	400	400	400	400	400	400	400	400	400	600	850
CO_2 regeneration rate, kg/h	78.9	74.9	69.6	69.1	67.3	65.9	71.2	79.9	72.1	86.2	83.9	99.6	90.1	98.1	96
Condenser T, °C	25.6	24.2	21.6	23.9	27.6	32	42.9	29.3	30	20.5	22.5	20.5	32.4	28.8	28.8
							Comparison of test results and simulation results								
Rich in T, °C	108.4	124.3	110.1	106.3	108.8	109.2	107.3	114	102.5	108.3	109.2	109.8	110.2	118.5	123.8
Exp. T, °C	119.4	139.1	122.8	118.8	121.8	120.5	119	126	113.7	120.8	124	120.8	124.3	133	140
Pred. T, °C	119	136.4	123.8	119.1	121.7	121.3	118.1	126.3	121.7	120.2	123.8	120.1	127	133.3	140.4
Exp. average, ppm	719	860	819	1019	2759	3339	n.a	3552	n.a	n.a	1625	n.a	n.a	n.a	1351
Pred.,ppm	1035	464	1085	1864	2675	4177	13815	3233	3919	1264	1531	1028	4516	2002	1101
Exp. (solvent), kW	145.7	176.9	98.9	97.7	98.8	90.5	95.5	102.1	81.3	108.2	100.4	133.8	101.9	124.4	130.6
Exp. (steam), kW	163.6	171.1	101.2	105.4	99.8	97.7	132.3	150.3	92	122.7	121.8	147.7	92.7	133.48	143.4
Pred., kW	142.2	158.8	112.3	107.9	109.5	104	100.6	124.1	114.6	118.9	110.4	147.8	124.2	137.5	134.9

More details on pilot plant trials can be found in Yu et al., 2012a

n.a = not available

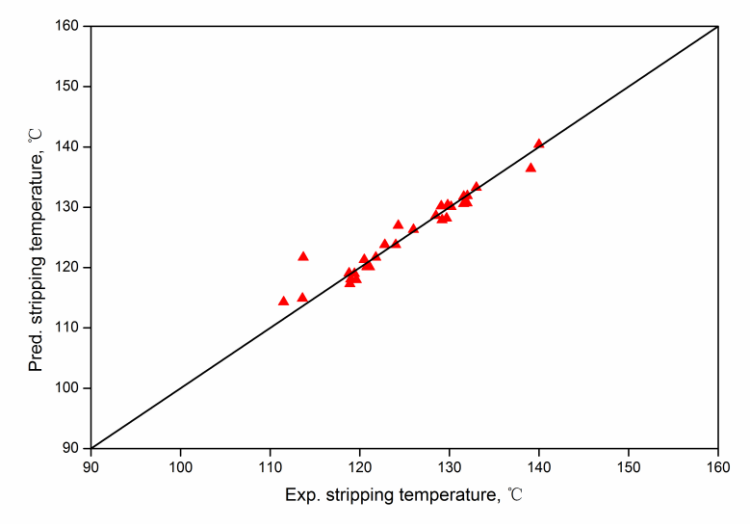

Figure 14 Parity plot of measured and predicted stripping temperature under conditions listed in Table 10

Figure 14 shows the parity plot of stripping temperature measured experimentally and obtained from simulation. The relative deviations between them are below 7% for all 30 cases considered, and below 3% in most cases.

Figure 15 shows the parity plot of the average value of ammonia concentration in product stream measured experimentally and the value obtained from simulation. Reasonable agreement has been achieved between the results.

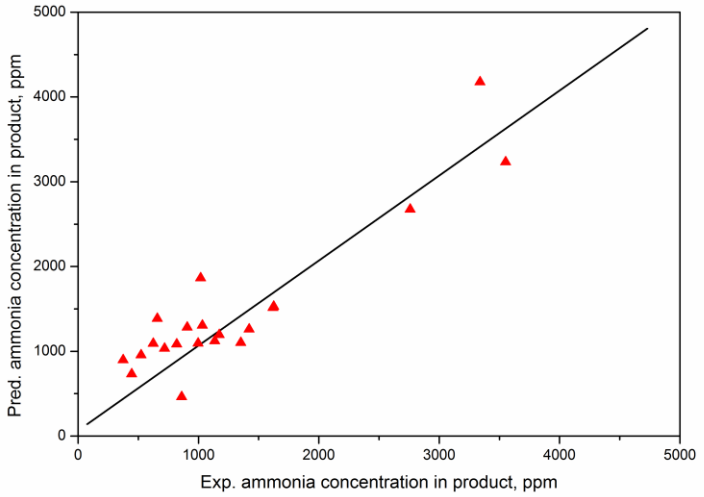

Figure 15 parity plot of the average value of ammonia concentration in product stream measured experimentally and the value obtained from simulation

(c) SO_2 removal by aqueous ammonia

The results from the dosing experiments are used to validate the model for the absorption of SO_2 by aqueous ammonia. The model settings for the pretreatment column were based on the conditions of pilot plant trials, including the column size, packed materials, operating conditions.

It is well-known that during the SO_2 absorption process, the oxidation process of S(IV) $\xrightarrow{O_2}$S(VI) inevitably occurs in the presence of oxygen. In our simulation, we assume that the SO_2 in the gas phase and SO_3^{2-} in aqueous solution are not oxidated by the oxygen during the capture process. This assumption is based on the following considerations (Miller, 1972; Hegg, 1978;McKay, 1971): (1) the oxidation of S(IV)→S(VI) primarily takes place in the liquid phase after SO_2 is dissolved into the solution generating SO_3^{2-} species, and thus the oxidation will have little influence on the SO_2 transportation from gas phase to liquid phase; (2) the oxidation rate of SO_3^{2-} to SO_4^{2-} is kinetically controlled and can be generally expressed as $\frac{d[SO_4^{2-}]}{d_t} = K[SO_3^{2-}]$. This means the rate of production of SO_4^{2-} is proportional to the concentration of SO_3^{2-} while in the pilot plant testing, the SO_3^{2-} concentration was very low and below 0.011 mol/L; [3] the SO_2 removal process was carried out in the oxygen-deficit environment due to the relatively low oxygen concentration below 8.0 % in the flue gas, which does not favor the oxidation process. Therefore the assumption will have a minor influence on the simulation of SO_2 removal by aqueous ammonia in the pilot plant. This is verified by the excellent agreement between model predictions and experimental results in terms of the solution pH, NH_3, SO_2 and CO_2 concentration at the pretreatment column outlet (Figure 16).

Outlet solution pH: Absorption of the acidic gas SO_2 into the aqueous solution will lead to a decrease of solution pH due to the low dissociation constant of H_2SO_3 (pKa=1.81). As shown in Figure 16(a), the solution pH dropped quickly with the SO_2 absorbed by the circulated water due to the increasing solution acidity. The pH value then increased step by step with the increasing ammonia dosing rate. The simulation curve matches experimental results very well. As the solution pH is a very important indication of the species distribution, the validation of solution pH to some extent reflects that the model enables the predication of the solution species in the system of NH_3-CO_2-SO_2-H_2O.

Gas outlet SO_2 concentration: The SO_2 level in the outlet flue gas directly reflects the SO_2 removal efficiency by aqueous ammonia. As shown in Figure 16(b), upon water circulation, the outlet SO_2 concentration experienced a rapid drop but quickly increased to a level close to the inlet SO_2 concentration. This implies that the fresh water has a relatively low SO_2 removal capacity. With the increasing NH_3 dosing rate over 0.5 kg/hr, the SO_2 concentration dropped to a very low level. The simulation results agree reasonably well with the experiment data at these NH_3 dosing stages.

Gas outlet ammonia concentration: The ammonia introduced into the water was used to neutralize the acidic gas SO_2. If the dosed ammonia was excessive for SO_2 absorption, part of ammonia will slip to the flue gas due to the intrinsic property of high volatility and high pH of the wash water. As shown in Figure 16(c), amonia started to slip at the dosing rate of 1.0 kg/hr NH_3, above which ammonia evaporation increased dramatically. The trend of outlet ammonia concentration is in good consistence with the modelling results.

Gas outlet CO_2 flow rate: As shown in Figure 16(d), there is no appreciable CO_2 removal in the test. This suggests that under the conditions studied, SO_2 is absorbed in the solution in preference to CO_2.The simulation results were in good agreement with the experimental results.

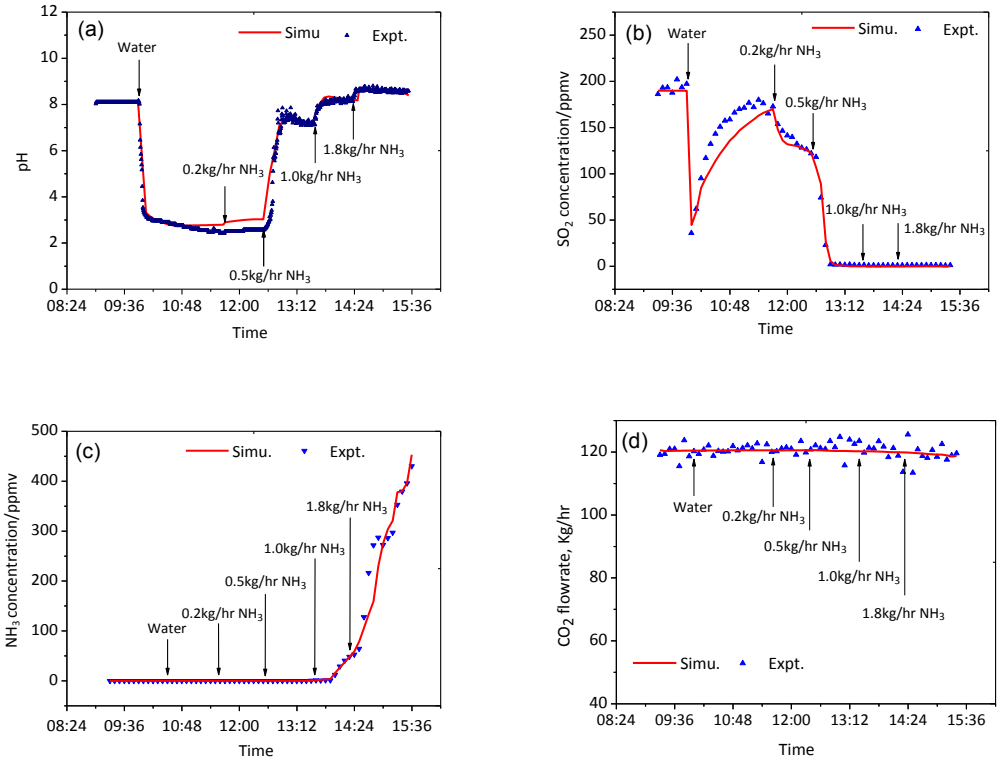

Figure 16 Comparison of pilot plant data with simulation results (a) solution pH; (b) gas SO_2 concentration; (c) gas ammonia concentration; (d) gas CO_2 flow rate outlet

The good agreement between the experimental and modelling results suggests that the established model can well predict the SO_2/CO_2 absorption process by aqueous ammonia. This, in turn, confirms that the assumptions are reasonable at the studied conditions.

6.2 Rate based modelling of SO_2 removal and NH_3 recycling

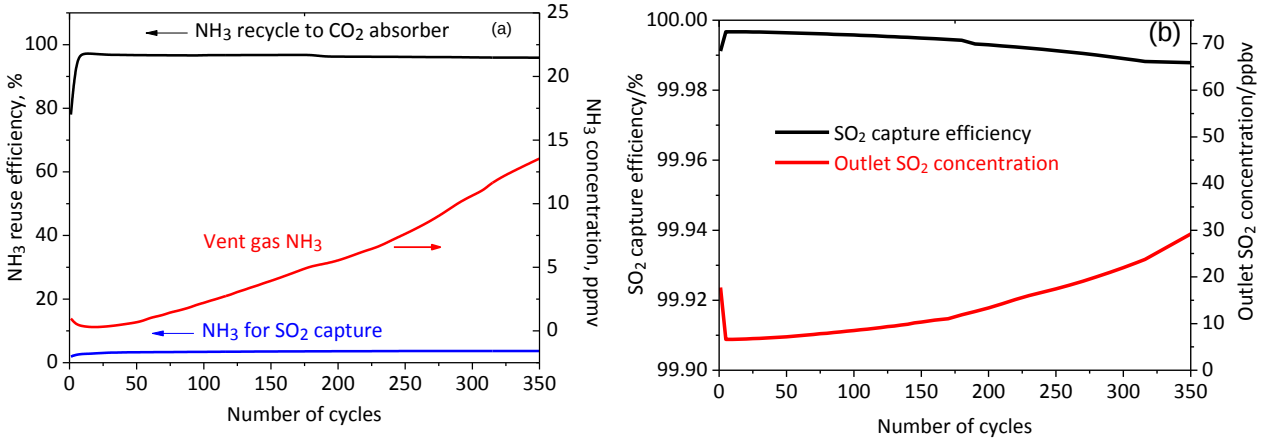

Figure 17 (a) NH_3 reuse efficiency and emission concentration (b) SO_2 removal efficiency and emission concentration as a function of number of cycles

Using the validated rate-based model, we simulated the proposed combined SO_2 removal and NH_3 recycle process under the conditions listed in section 4.2. Figure 17 shows the ammonia reuse efficiency and SO_2 removal efficiency as a function of number of cycles. The ammonia slipped from the CO_2 absorber was

either reused (recycled back to the CO_2 absorber or remain in the wash water for SO_2 removal) or emitted in the combined SO_2 removal and NH_3 recycle system. Ammonia reuse efficiency (removal efficiency) is defined as percentage of ammonia which is recycled back to the CO_2 absorber and remains in the wash water. At steady state 96.62% of ammonia was recycled to CO_2 absorber, while 3.36% of ammonia was used for SO_2 capture. So the total ammonia reuse efficiency reached as high as 99.98%.

Figure 17(b) shows that the proposed process achieved a high SO_2 capture efficiency constantly over 99.98% and the SO_2 emission concentration was in trace level varied from 10 ppbv to 30 ppbv. This high efficiency removal is primarily attributed to the fast reaction between SO_2 and H_2O and the fact that the generated HSO_3^- was quickly neutralized by basic aqueous ammonia.

Figure 18 shows the concentration profiles of sulfur-containing species in wash water at the outlet of the pretreatment column as a function of number of cycles. SO_2 and ammonia were accumulated in the solution in the forms of $(NH_4)_2SO_3$, NH_4HSO_3 and $(NH_4)_2S_2O_5$. $(NH_4)_2SO_3$ was persistently the dominant species in the wash water and the concentration increased gradually to 35% (saturated concentration of $(NH_4)_2SO_3$ at 10 ^oC) while the NH_4HSO_3 and $(NH_4)_2S_2O_5$ remained at relatively low levels. The concentrated SO_2 solution is expected to undergo a further treatment, e.g. producing ammonium sulfite/sulfate fertilizers. It should be pointed out that CO_2 was not absorbed in the combined capture process. In other words, the process achieves selective removal of SO_2 and ammonia in preference to CO_2.

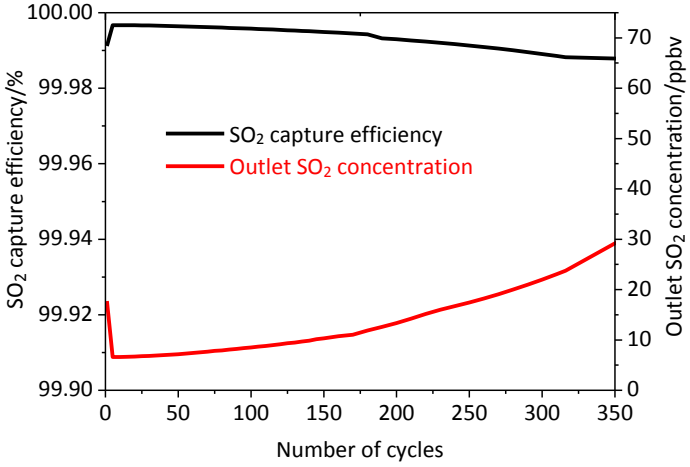

Figure 18 Concentration of major SO_2 containing species at the pretreatment column outlet as a function of number of cycles

Wash column

To gain the insight of how the ammonia is removed, the wash column profiles with respect to the ammonia removal efficiency and temperature were studied. The vaporised ammonia from CO_2 absorber was scrubbed in the wash column using the circulated ammonium sulphite solution. As shown in the Figure 19 (a), the ammonia removal efficiency increases along the packed column and the value can reach over 99.9%. This means that almost all the slipped ammonia was scrubbed in the solution in the forms of free ammonia and NH_4^+ ion species.

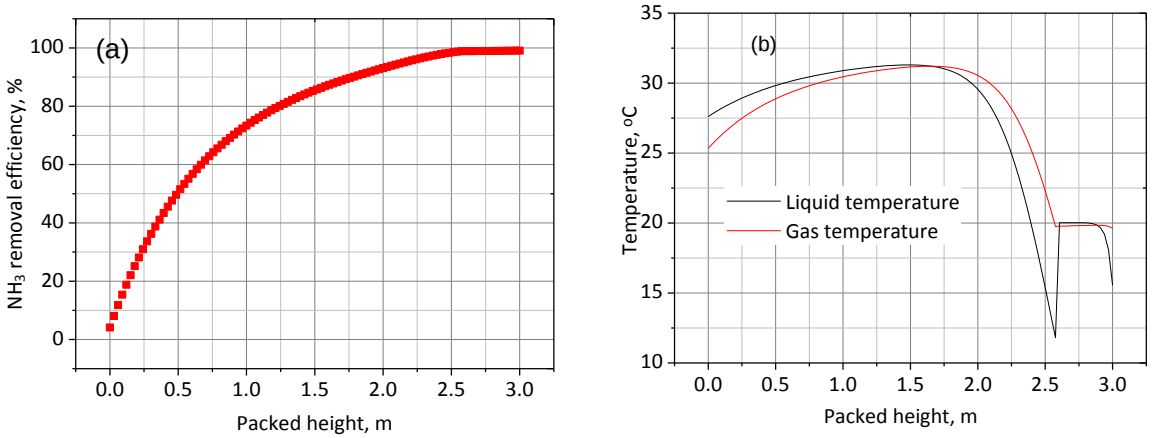

Figure 19 (a) NH_3 removal efficiency and (b) temperature profile as a function of packed height

It is well known that the NH_3 absorption by aqueous solution is an exothermic process, leading to an overall temperature increase of the solution (Figure 19 (b)). This will decrease the NH_3 solubility in the solvent and reduce the driving force for ammonia absorption. So the low temperature is required in order to achieve a high removal efficiency for ammonia. In this simulation, the 10 ^oC wash water was used to obtain a high ammonia removal efficiency. The liquid temperature profile along the column experienced two peaks. One was caused by the exothermic process of NH_3 absorption by the wash solution. The other was caused by the 10 ^oC fresh makeup water that was introduced into the top of washing column. The makeup water played two roles: One was to maintain the H_2O balance of the system; the second was to have a deep removal of NH_3. The simulated temperature profile shows that the liquid temperature ranged from 10 ^oC to 32 ^oC in the wash column. This temperature range provides the reference for the separate NH_3 absorption in the bubble column.

Pretreatment column

After the slipped NH_3 was absorbed in the wash column, the solution was sent to the pretreatment column which played three significant roles in the proposed SO_2 removal and NH_3 recycle process. The first was to cool down the high temperature flue gas from power station. As shown in Figure 20 (a), the flue gas temperature experienced a sharp decrease after contact with the relatively low temperature solvent along the packed column. The outlet gas temperature from the pretreatment column decreased to 43.6 ^oC and the gas can be directly transported to the CO_2 absorber without further cooling. Our simulation has confirmed that the flue gas temperature from 15 ^oC to 50 ^oC had little influence on the CO_2 absorption process including absorption rate and ammonia vaporization rate. This is due to the small heat capacity of the gas and the fact that the latent heat in the high temperature flue gas has been released and transferred to the solvent.

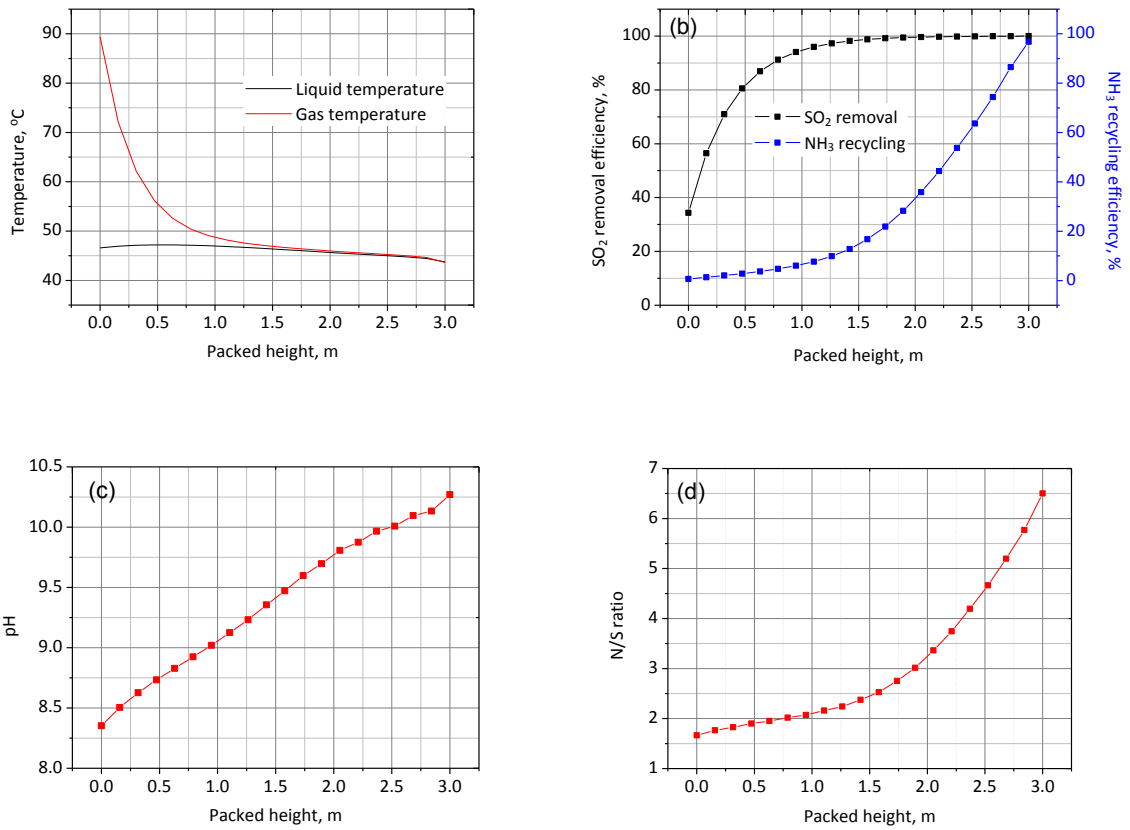

Figure 20 (a) liquid and gas temperature profile, (b) SO_2 removal efficiency and NH_3 recycling efficiency, (c) solution pH profile, (d) N/S ratio profile as a function of the packed height

The second role was to remove the SO_2 in the flue gas. The result in Figure 20(b) shows that SO_2 removal efficiency increased sharply to 95% in the first 1.0 m packed height and slightly in the remaining 2. 0 m packing.

The third role was to recycle the scrubbed ammonia to the CO_2 absorber by making use of latent heat in the flue gas. As shown in Figure 20(b), the NH_3 recycling (reuse) efficiency increased steadily along the column and reached the maximum of 99.9% at the top of column. In the pretreatment column, the solution was heated by the high temperature flue gas and released the NH_3 vapor. The solution pH decreased as the wash water flowed down along the column, as shown in Figure 20(c). The decrease was due to the absorption of SO_2 and evaporation of ammonia. Figure 20(d) describes the N/S ratio profile in the liquid phase (the molar ratio of N-containing species to the S-containing species) as a function of packing height. Initially, the solution at the column top contained the free NH_3 and had a high N/S ratio. With the liquid falling down along the column, the ratio decreased gradually due to the release of molecular NH_3 from the solution. The vaporized ammonia was then recycled back to the CO_2 absorber as make up. It is worth mentioning that the N/S ratio can be below 2.0 at the bottom stage. This implies that all the free ammonia was recycled and part of $(NH_4)_2SO_3$ was decomposed to release the NH_3 vapor. The decomposition of $(NH_4)_2SO_3$ occurring at the column bottom was partly attributed to the high temperature flue gas in the bottom stage (Figure 20(a)).

In summary, the multi-function pretreatment column acted as: (1) a cooler to cool down the high temperature flue gas; (2) a heater to recycle almost all the escaped NH_3 to the CO_2 absorber; and (3) an

efficient desulphurization facility to deeply remove SO_2. Accordingly, this advanced process would hold the advantages of (1) saving the energy consumption for the flue gas cooling; (2) reducing the energy and capital cost for the NH_3 recovery system; (3) and simplifying the flue gas desulphurization (FGD) process which is particularly important in Australia as the FGD system is not installed in Australian power plants.

6.3 SO_2 and ammonia absorption experiments

Based on the modelling results, the experimental work using bubble column was carried out to qualitatively verify the prediction results on SO_2 and ammonia absorption separately.

6.3.1. SO_2 absorption and NH_3 vaporization

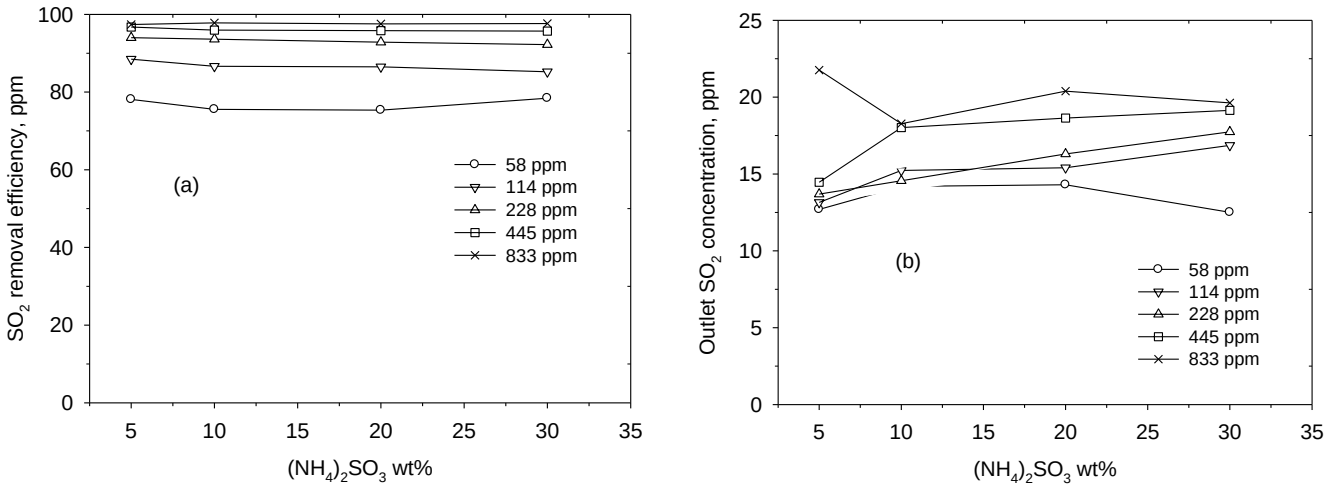

Figure 21 (a) SO_2 and CO_2 removal efficiency and (b) SO_2 concentration at the column outlet as a function of $(NH_4)_2SO_3$ concentration at various SO_2 inlet concentrations and the temperature of 313 k (40°C).

The modelling results in Section 6.2 suggests that the SO_2 absorption process was performed in the liquid temperature range of 42-48 °C. The temperature of 40 °C was used to test the SO_2 absorption in the bubble column. The SO_2 inlet concentration varied from 58 ppmv to 833 ppmv, which covers the typical SO_2 level in the flue gas from Australian coal-fired power stations. As shown in Figure 21(a), the $(NH_4)_2SO_3$ solution had excellent SO_2 removal efficiency for the high SO_2 level flue gas, while a relatively low SO_2 removal efficiency for the low SO_2 level flue gas. Figure 21 (b) shows that the outlet SO_2 concentrations from the bubble column were very small, generally below 20 ppm. The values changed little with variation of $(NH_4)_2SO_3$ concentration and increased slightly with an increase in inlet SO_2. This means the $(NH_4)_2SO_3$ concentration has a high SO_2 absorption capacity. It should be pointed out that the CO_2 removal efficiencies were negligible under all conditions studied. One of examples is shown in Figure 22 which shows the SO_2 and CO_2 removal efficiency and outlet ammonia concentration as a function of $(NH_4)_2SO_3$ concentration at two temperatures (25°C and 40°C) and inlet SO_2 concentration of 445 ppm. There was virtually no CO_2 removal while SO_2 removal efficiencies were above 95% and slightly higher at low temperatures. This clearly indicates that the $(NH_4)_2SO_3$ solutions can selectively remove SO_2 in preference to CO_2.

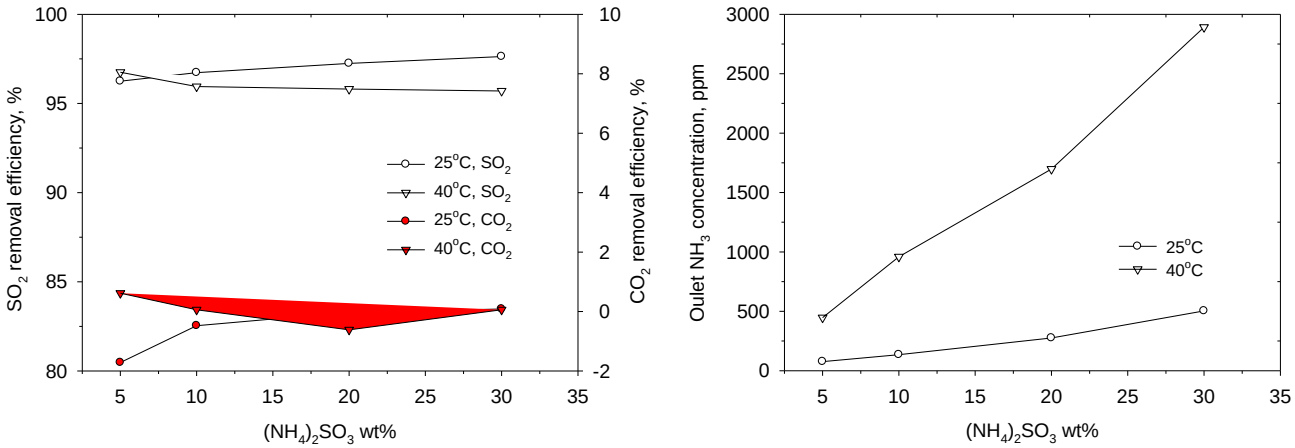

Figure 22 (a) SO_2 and CO_2 removal efficiency and (b) outlet NH_3 concentration as a function of $(NH_4)_2SO_3$ concentration at two temperatures (25°C and 40°C) and inlet SO_2 concentration of 445 ppm. CO_2 inlet concentration was 10.4 %

Figure 22 (b) shows the ammonia evaporation occurred in the SO_2 absorption process and the amount of NH_3 in the gas increased with increasing $(NH_4)_2SO_3$ concentration, in particular with increasing temperature This suggests that high temperature absorption does not affect SO_2 and CO_2 removal but significantly facilitate ammonia evaporation and thus its recycle.

6.3.2 NH_3 absorption

The modelling results in Section 6.2 show that the ammonia absorption process occurred at temperatures between 10 and 32 °C. 10 °C and 25 °C were selected to represent the temperature swing during absorption process.

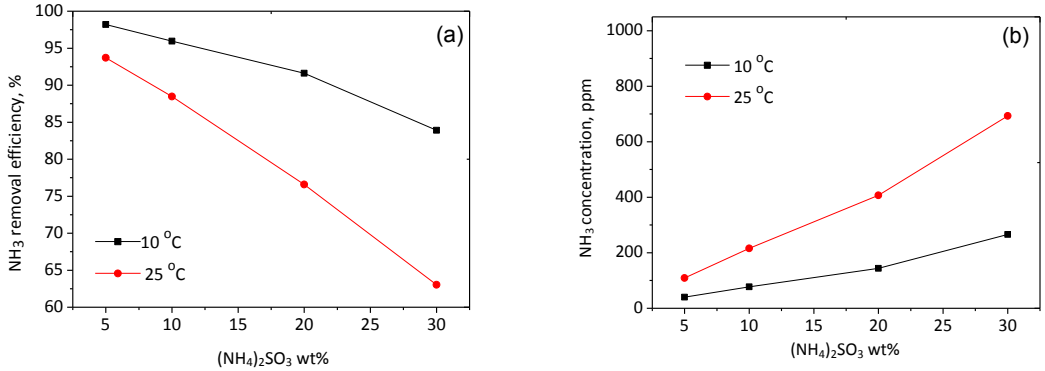

Figure 23 (a) NH_3 removal efficiency and (b) NH_3 concentration at the column outlet as a function of $(NH_4)_2SO_3$ concentration at 10 and 25°C. NH_3 concentration at the inlet is ca. 2000 ppm and CO_2 inlet concentration was 2.0%

Figures 23 shows the ammonia removal efficiency and ammonia concentration at the column outlet as a function of $(NH_4)_2SO_3$ concentration at 10 and 25°C respectively. It is evident that the ammonia removal efficiency decreased and the corresponding NH_3 concentration at the column outlet increased with an

increase in $(NH_4)_2SO_3$ concentration. The ammonia removal efficiency was over 85% at 10 ^oC, while at 25 ^oC the absorption efficiency drop significantly, especially at high $(NH_4)_2SO_3$ concentrations.

The experiments proved the concept of the combined capture process and demonstrated the feasibility of SO_2 removal and ammonia recycling through the application of the proposed process configuration.

6.4 Solvent development

The previous results have showed that both amino acid salts including sarcoinate and prolinate, piperazine and its derivatives including 1-methyl piperzaine and 2 methy piperazine can promote NH_3 absorption. The promotion mechanism has been elucidated by stopped flow kinetic study of the reaction of CO_2 with ammonia, promoters and ammonia/promoter mixture. The previous study has also showed that the reaction of CO_2 with ammonia/promoter mixture is a simply combination of the two individual reaction system and there is no catalytic effect from promoters. In other words, the promoter itself acts as a reactant and can react with CO_2 in a similar way to ammonia. These promoters have much higher reaction kinetics with CO_2 than ammonia, which is the major reason why introduction of these promoters can significantly enhance CO_2 absorption in aqueous NH_3. In case of amino acid salts, the extent of promotion is pronounced at low CO_2 loadings but becomes smaller with an increase in CO_2 loading. Figure 24 shows the mass transfer coefficient of CO_2 in the mixture of ammonia with potassium prolinate as a function of CO_2 loading at the temperature of 288 K. For comparison purpose, the mass transfer coefficient of CO_2 in 3 M NH_3 and 30% MEA are included.

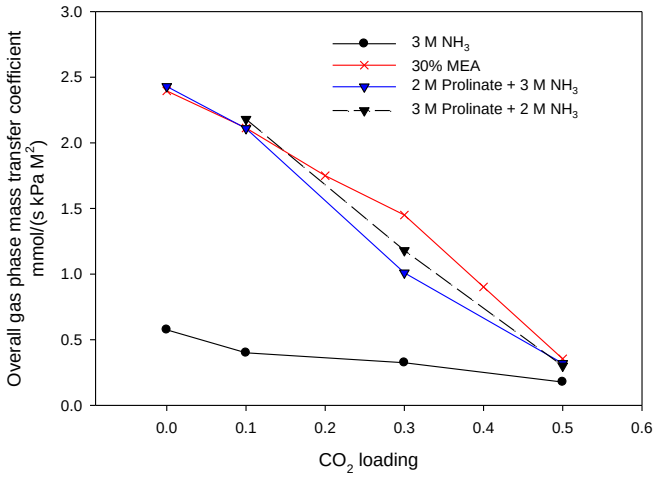

Figure 24 Mass transfer coefficient of CO_2 in the mixture of ammonia with potassium prolinate as a function of CO_2 loading at the temperature of 288 K. The data for 30% MEA was obtained at 313 K

At CO_2 loadings below 0.1, the mass transfer coefficients of CO_2 in both 2 M prolinate/3 MNH_3 and 3 M prolinate/2M NH_3 match those in MEA. But the values drop rapidly with an increases in CO_2 loading and are lower those in MEA at CO_2 loadings between 0.1 and 0.5. At loadings close to 0.5, mass transfer coefficients in all solutions are similar. Similar results were observed in sarcoinate/NH_3 mixture, as reported previously.

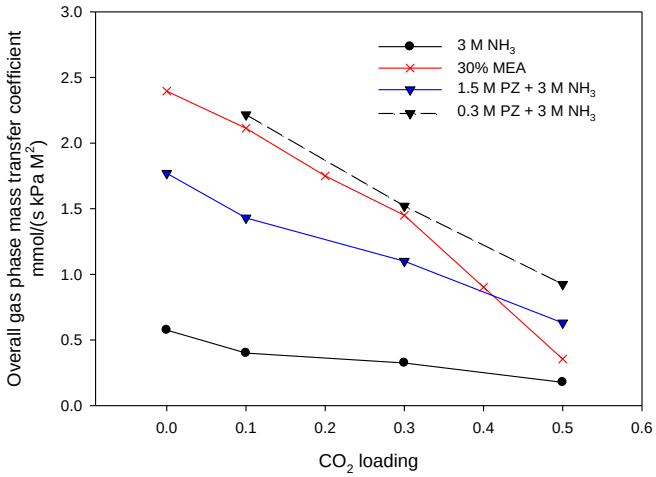

Figure 25 Mass transfer coefficient of CO_2 in the mixture of ammonia with piperazine as a function of CO_2 loading at the temperature of 288 K. The data for 30% MEA was obtained at 313 K

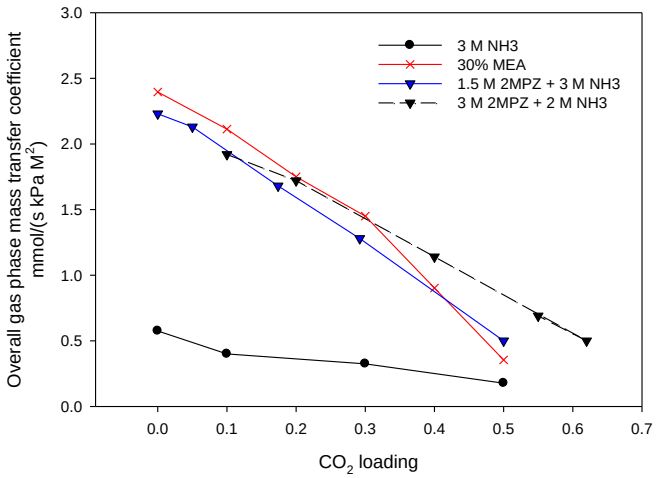

Figure 26 Mass transfer coefficient of CO_2 in the mixture of ammonia with 2-methyl piperazine as a function of CO_2 loading at the temperature of 288 K. The data for 30% MEA was obtained at 313 K

Figures 25 and 26 show mass transfer coefficients of CO_2 in the mixture of ammonia with piperazine and ammonia with 2-methyl piperazine as a function of CO_2 loading at the temperature of 288 K respectively. Mass transfer coefficient of CO_2 in 1.5 piperazine/3 M ammonia mixture and 3 M 2-methyl piperazine/2 M ammonia can match those in MEA in a wide CO_2 loading range. As discussed in the previous reports, these diamines have two advantages. One is that these amines have 2 amino functional groups both of which react with CO_2 faster than ammonia, thus enhancing CO_2 absorption at CO_2 loaded solutions. pKa values of these amines are close or even lower than that of ammonia. Protons released from the CO_2 dissolution or depronotation of carbamic acid can react with ammonia in preference to amines. So more free amines are available to react with CO_2. While in case of sarcosinate and prolinate, pKa of these amino acid salts are much higher than ammonia and have only one amino group. With an increase in CO_2 loading (amount of CO_2 in the solution), the concentration of the free amino acid salts in amino acid salts/ammonia mixture decrease to a larger extent than those in the single amine and the role of these amino acid salts in promotion of CO_2 absorption becomes much smaller.

So it can be concluded that the amino acid salts studied in this work can significantly enhance CO_2 absorption in aqueous ammonia at low CO_2 loadings but their role in promotion of CO_2 absorption rate becomes much smaller with an increase in CO_2 loading. The mass transfer coefficients of CO_2 in amino acid salts and NH_3 mxitures are close to those in MEA but generally lower under the conditions studied. In comparison, ammonia with piperazine or 2-methyl piperazine can achieve mass transfer coefficients higher than those in MEA. Our focus on the solvent development in this project will be piperazine or 2-methyl piperazine promoted ammonia solution. We are currently developing rate-based models for the piperazine-NH_3-CO_2-H_2O system and 2-methyl piperazine-NH_3-CO_2-H_2O system. The available of models will allow evaluation of the performance of the piperazine or 2-methyl piperazine based capture process.

6.5 **Modelling of CO_2 absorption in piperzaine/ammonia mixture in a wetted wall column**

Estimated values of K_G are compared to wetted-wall measured values in Figure 27. This comparison is for various piperazine concentrations and a constant CO_2 concentration of 0.9 M. When using the value of k_7 (the rate constant for the forward reaction of ammonia with CO_2) from Wang et al.(2011) in the calculations (determined by stopped-flow spectrometry at low NH_3 concentration, 469 $M^{-1}.s^{-1}$), the calculated K_G values underestimate the measured K_G by a relative error of approximately 30-40%. Alternatively, when using a value of k_7 determined from two previous studies using a similar wetted-wall column to that used in this work (1170 $M^{-1}.s^{-1}$ (Li et al., 2013), and 3369 $M^{-1}.s^{-1}$ (Puxty et al., 2010), the calculated K_G values are in closer agreement to the measured values. When using the smaller value of the two, the agreement is better at lower piperazine concentrations, and when using the larger value, a better agreement is achieved at higher piperazine concentrations. The reason for this discrepancy is not clear. Of the k_7 values, that determined in a homogeneous single phase by stopped-flow spectrometry is likely the most reliable as the assumptions and errors introduced when studying gas-liquid reactions are eliminated. However, this determination was done at mM (millmolar) NH_3 concentrations rather than the M (molar) concentrations used in the wetted-wall studies. The larger k_7 values determined in the wetted-wall studies could be due to the volatility of NH_3 leading to additional reaction occurring at the gas-liquid interface or in the gas phase that is not captured in the mass transfer simulations. Further investigation is required to understand the reasons for the discrepancy and improve the mass transfer simulations.

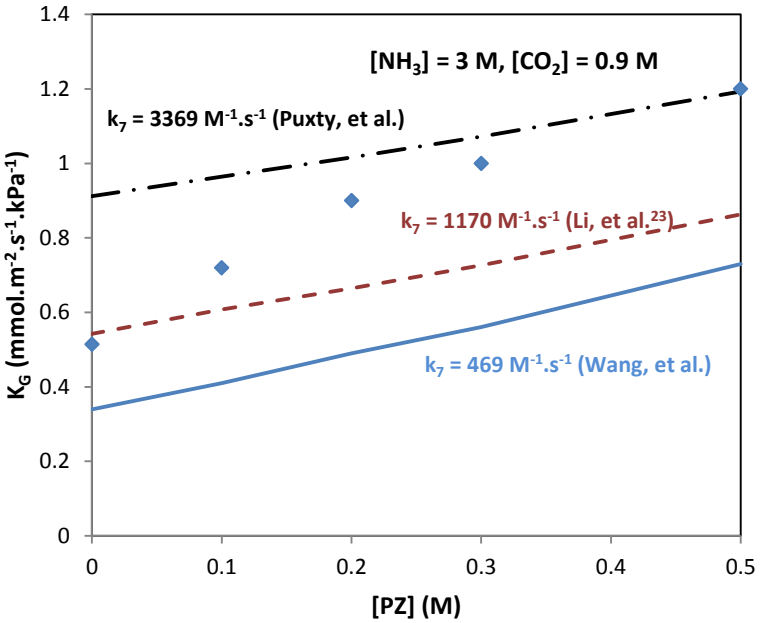

Figure 27 The mass transfer model estimated value of K_G (solid lines) compared to the wetted-wall measured values (diamonds) for different concentrations of PZ at a constant CO_2 loading of $[CO_2]/[NH_3]$ = 0.3 and using different values of k_7

It should be noted that, for both calculated and experimental values listed in Figure 27, K_G increases with the concentration of piperazine added to the blended ammonia/piperazine solutions with constant ammonia and CO_2 concentrations in solutions. The reason for the increase is the increasing contribution from the reaction of CO_2 with PZ/PZH^+ and $PZCO_2^-/PZCO_2H$ as outlined in the last progress report.

6.6 Impact of research achievements from this project

The research has so far led to the following advancements:

(1) Development of a rigorous rate-based model for the system of NH_3-CO_2-SO_2-H_2O. The model has been validated using the experimental results from open literature and pilot plant trials at Munmorah Power Station.

(2) Development of a combined SO_2 removal and NH_3 recycle process which can be integrated with the aqueous ammonia based CO_2 capture process.

(3) Development of aqueous ammonia based solvents which can match MEA based solvents in terms of CO_2 absorption rate. Ammonia blended with piperazine or 2-methyl piperazine can achieve mass transfer coefficients higher than those in MEA.

The availability of the rigorous rate-based model will allow a reliable process evaluation and guide process improvement and optimisation. The combined SO_2 removal and NH_3 recycle process can simply the flue gas desulphurization (FGD) process, save the energy consumption for the flue gas cooling and reducing the energy and capital cost for the NH_3 recovery system. Currently we are assessing the technical and energy performance of an advanced aqueous ammonia-based CO_2 capture technology for a 500 MW coal fired power station and comparing the energy consumption with those in chilled ammonia process and MEA based process (Li, 2014). The technology is still based on aqueous ammonia (no promoters are

added) but includes the combined SO_2 removal and NH_3 recycle process. It has been found that the advanced ammonia based process has a net efficiency penalty of 7.9 % points, which is lower than that for modified CAP process (8.5%) and much lower than that for the MEA process (10.9%). The results will be reported in the following reports.

Development of aqueous ammonia based solvents which can match MEA based solvents in terms of CO_2 absorption rate can significantly reduce the column size and the capital costs associated with the ammonia based capture process. We are currently developing rate-based models for the piperazine-NH_3-CO_2-H_2O system and 2-methyl piperazine-NH_3-CO_2-H_2O system. The models will allow a more realistic evaluation of the performance of the piperazine or 2-methyl piperazine promoted ammonia capture processes.

References

Aspen Technology, 2010. Aspen physical property system: physical property models. Burlington, MA, USA.

GÖppert U.; Maurer G., 1988. Vapor-liquid equilibria in aqueous solutions of ammonia and carbon dioxide at temperatures between 333 and 393 K and pressures up to 7 MPa. Fluid Phase Equilibria, 41, 153-185.

Hegg, D.A. and Hobbs, P.V., 1978, Oxidation of sulfur dioxide in aqueous systems with particular reference to the atmosphere, Atmospheric Environment, 12, 241-253.

Kurz F.; Rumpf B.; Maurer G. 1995. Vapor-liquid-solid equilibria in the system NH_3-CO_2-H_2O from around 310 to 470 K: New experimental data and modeling. 104, 261-275.

Lichtfers, U., 2000. Spectroscopic studies for the determination of species distributions in the system ammonia - carbon dioxide – water, Ph.D. thesis, Kaiserslautern University.

Li, K.K., Yu, H., Feron, P., Tade, M., Wardhaugh, L., 2014. An assessment of technical and energy performance of an advanced aqueous ammonia-based CO_2 capture technology for a 500 MW coal fired power station, paper manuscript to be submitted to Applied Energy**.**

Li, L., Han, W., Yu, H., Tang, H.,2013. CO_2 absorption by piperazine promoted aqueous ammonia solution: absorption kinetics and ammonia loss. Greenhouse Gases: Science and Technology.

McKay, H.A.C., 1971. The atmospheric oxidation of sulphur dioxide in water droplets in presence of ammonia, Atmospheric Environment, 5, 7-14.

Qi, G.J., 2014. Ph.D. thesis, Tsinghua University.

Qi, G.J.; Wang, S.J.; Yu, H.; Wardhaugh, L.; Feron, P. ;Chen C.H., 2013. Development of a rate-based model for CO_2 absorption using aqueous NH_3 in a packed column, International Journal of Greenhouse Gas Control, 17, 450–461.

Puxty, G., Rowland, R. 2011. Modeling CO_2 mass transfer in amine mixtures: PZ-AMP and PZ-MDEA, Environmental Science & Technology 45, 2398-2405.

Scott W.D. and McCarthy, L., 1967. The system sulfur dioxide-ammonia-water at 25° C, Industrial & Engineering Chemistry Fundamentals, 6, 40-48.

Yu, H., Qi, G., Wang, S., Morgan, Allport, A., Cottrell, A., Do, T., McGregor, J., Wardhaugh, L., Feron, P., 2012a, Results from trialling aqueous NH_3 based post combustion capture in a pilot plant at Munmorah Power Station: Solvent regeneration energy. Chemeca 2012: Quality of life through chemical engineering: 23–26 September 2012, Wellington, New Zealand, 2012a: 1097.

Yu, H., Morgan, Allport, A., Cottrell, A., Do, T., McGregor, J., Wardhaugh, L., Feron, P., 2012b. Results from trialing aqueous ammonia-based post-combustion capture in a pilot plant at Munmorah Power Station: Gas purity and solid precipitation in the stripper. International Journal of Greenhouse Gas Control, 10, 15–25.

Miller J.M. and DePena, R. 1972, Contribution of scavenged sulfur dioxide to the sulfate content of rain water**,** Journal of Geophysical Research, 77, 5905-5916.

Wang, X., Conway, W., Fernandes, D., Lawrance, G., Burns, R., Puxty, G., Maeder, M., 2011. Kinetics of the reversible reaction of CO_2(aq) with ammonia in aqueous solution. The Journal of Physical Chemistry A 115, 6405-6412.

7 Conclusions

The project has made a good progress and has completed the milestones listed in the reporting period.

Using Aspen Plus®, we have developed a rigorous rate-based model for the system of NH_3-CO_2-SO_2-H_2O and validated the model against the experimental results from open literature and pilot plant trials at Munmorah Power Station. The model can satisfactorily predict the CO_2 absorption, CO_2 desorption and SO_2 removal processes in packed columns and thus guide process evaluation and optimisation.

We have proposed a novel process to combine SO_2 removal and ammonia recycling. The process can be integrated with the aqueous ammonia based CO_2 capture process to achieve flue gas cooling, SO_2 and CO_2 removal and ammonia recycle simultaneously in one process. The process simulation using the rated-based model shows that under the typical flue gas conditions, the proposed process has a SO_2 removal efficiency of over 99.9% and an ammonia reuse efficiency of 99.9%. The novel process can not only simplify the flue gas desulfurization, but also resolve the problems of ammonia loss and SO_2 removal, thus holding the potential of cutting the CO_2 capture costs significantly. The separate experiments on SO_2 and ammonia absorption using a bubble column were carried out to further evaluate the technical feasibility of the combined SO_2 removal and ammonia recycling process. The experimental results qualitatively confirmed the simulated results and the technical feasibility of the process.

In terms of solvent development, the amino acid salts studied in this work can significantly enhance CO_2 absorption in aqueous ammonia at low CO_2 loadings but their role in promotion of CO_2 absorption rate becomes much smaller with an increase in CO_2 loading. The mass transfer coefficients of CO_2 in amino acid salts and ammonia mixtures are close to those in MEA but generally lower under the conditions studied. In comparison, ammonia mixed with piperazine or 2-methyl piperazine can achieve mass transfer coefficients higher than those in MEA.

In an attempt to develop a rate-based model for the promoted ammonia solvents which is not available in Aspen Plus, we used an in-house software tool implemented in the Matlab® to model the mass transfer of CO_2 in the ammonia and piperazine mixtures in a wetted wall column. The software tool incorporates the reaction kinetic model developed from stopped flow kinetic study and solves partial differential equations and nonlinear simultaneous equations that define the diffusion, reaction and equilibrium processes occurring in a thin liquid film. It has been found that both calculated and experimental mass transfer coefficients increases with the concentration of piperazine added to the blended ammonia/piperazine solutions with constant ammonia and CO_2 concentrations in solutions. However, the calculated values underestimate the measured values by a relative error of approximately 30-40%. Further investigation is required to understand the reasons for the discrepancy and improve the mass transfer simulations.

The milestones of the project for the report period have been achieved and the project is on track to achieve the milestones which are due on 30 March 2015.

8 Future work

In the next 6 months, we will follow the plan specified in the proposal and carry out the following work:

- Use the developed rate-based model to assess the technical and energy performance of an aqueous ammonia-based CO_2 capture technology for a 500 MW coal fired power station and comparing the energy consumption with those in chilled ammonia process and MEA based processes. The technolgy integrates the combined SO_2 removal and NH_3 recyle with the capture process.
- Develop rate-based models for the piperazine-NH_3-CO_2-H_2O system and 2-methyl piperazine-NH_3-CO_2-H_2O system. The models will allow a more realistic evaluation of the performance of the piperazine or 2-methyl piperazine promoted ammonia capture processes. In addition, we will use the model to assess the performance of a complete CO_2 absorption system and identify the optimal conditions to be used for the demonstration of the advanced aqueous ammonia based PCC at a CO_2 capture rate of at least 10 kg/h with CSIRO's process development facility at Newcastle.
- Carry out the experiments on CO_2 absroption under pressure and investigate the effect of pressure on CO_2 mass trasnfer and ammonia loss.